Received: 9 December 2020 | Revised: 26 January 2021 | Accepted: 27 January 2021

DOI: 10.1111/mmi.14689

RESEARCH ARTICLE

WILEY

Consequences of producing DNA gyrase from a synthetic *gyrBA* operon in *Salmonella enterica* serovar Typhimurium

German Pozdeev | **Aalap Mogre** | **Charles J. Dorman**

Department of Microbiology, Moyne Institute of Preventive Medicine, Trinity College Dublin, Dublin 2, Ireland

Correspondence
Charles J. Dorman, Department of Microbiology, Moyne Institute of Preventive Medicine, Trinity College Dublin, Dublin 2, Ireland.
Email: cjdorman@tcd.ie

Funding information
Science Foundation Ireland, Grant/Award Number: Investigator Award 13/IA/1875

Abstract

DNA gyrase is an essential type II topoisomerase that is composed of two subunits, GyrA and GyrB, and has an A_2B_2 structure. Although the A and B subunits are required in equal proportions to form DNA gyrase, the *gyrA* and *gyrB* genes that encode them in *Salmonella* (and in many other bacteria) are at separate locations on the chromosome, are under separate transcriptional control, and are present in different copy numbers in rapidly growing bacteria. In wild-type *Salmonella*, *gyrA* is near the chromosome's replication terminus, while *gyrB* is near the origin. We generated a synthetic *gyrBA* operon at the *oriC*-proximal location of *gyrB* to test the significance of the gyrase gene position for *Salmonella* physiology. Although the strain producing gyrase from an operon had a modest alteration to its DNA supercoiling set points, most housekeeping functions were unaffected. However, its SPI-2 virulence genes were expressed at a reduced level and its survival was reduced in macrophage. Our data reveal that the horizontally acquired SPI-2 genes have a greater sensitivity to disturbance of DNA topology than the core genome and we discuss its significance in the context of *Salmonella* genome evolution and the *gyrA* and *gyrB* gene arrangements found in other bacteria.

KEYWORDS

DNA gyrase, DNA supercoiling, *gyrA*, *gyrB*, *Salmonella enterica* serovar Typhimurium, SPI-1, SPI-2

1 | INTRODUCTION

DNA gyrase is an essential type II topoisomerase that introduces negative supercoils into DNA through an ATP-dependent mechanism (Gellert et al., 1976a; Higgins et al., 1978; Nöllmann et al., 2007); it can also relax negatively supercoiled DNA via an ATP-independent mechanism (Gellert et al., 1977; Higgins et al., 1978; Williams & Maxwell, 1999). The enzyme is composed of two copies of two subunits, GyrA and GyrB, giving it an A_2B_2 structure (Bates & Maxwell, 2005). Gyrase binds to DNA, makes a double-stranded cut, with 4-base overhangs, in the "Gate" (or G) segment of the DNA, and passes a nearby "Transported" (or T) segment of intact DNA through the gap, changing the linking number of the DNA. The GyrA subunits form covalent bonds to the single-stranded DNA overhangs via tyrosine amino acids in their active sites, while the GyrB subunits bind and hydrolyze ATP (Corbett & Berger, 2004).

Topoisomerase activity is required to eliminate the over-wound (positively supercoiled) and under-wound (negatively supercoiled) zones of the DNA template that are generated by transcription and DNA replication (Liu & Wang, 1987; Stracy et al., 2019). DNA gyrase relaxes the positively supercoiled DNA by introducing negative supercoils in an ATP-dependent manner (Ashley et al., 2017). Transcription and the associated disturbance to local DNA topology contribute to the architecture of the bacterial nucleoid by influencing the probability of DNA-DNA contacts between parts of the genome that border long transcription units that are heavily transcribed (Le &

Laub, 2016). The changes in local DNA supercoiling that are caused by transcription and DNA replication also affect the activities of some transcription promoters (Ahmed et al., 2016, 2017; Chong et al., 2014; Dorman, 2019; Higgins, 2014; Rahmouni & Wells, 1992; Rani & Nagaraja, 2019; Tobe et al., 1995; Wu et al., 1988).

The in vivo superhelical density of DNA in *Escherichia coli* is −0.025 (Bliska & Cozzarelli, 1987) and it has been estimated that the DNA of *E. coli* has 15% more supercoils than that of *Salmonella enterica* serovar Typhimurium (Champion & Higgins, 2007). Because a large subset of promoters is sensitive to alterations in DNA supercoiling and, to ensure appropriate gene expression, topoisomerases are thought to play an important role in maintaining supercoiling set points within a range that is tolerable by the DNA transactions of the cell (Cheung et al., 2003; Dorman & Dorman, 2016; Peter et al., 2004; Sutormin et al., 2019). The promoters of *gyrA* and *gyrB*, the genes that encode the A and B subunits, respectively, of DNA gyrase, are stimulated by DNA relaxation (Menzel & Gellert, 1983, 1987; Straney et al., 1994; Unniraman & Nagaraja, 1999). This is part of a mechanism that maintains DNA supercoiling homeostasis, keeping average DNA supercoiling values within the tolerable range (DiNardo et al., 1982; Dorman et al., 1989; Pruss et al., 1982; Raji et al., 1985; Richardson et al., 1988; Steck et al., 1984). As a corollary to this, the transcription of *topA*, the gene encoding DNA topoisomerase I (Topo I), is stimulated by negative supercoiling (Ahmed et al., 2016; Tse-Dinh & Beran, 1988). Topo I relaxes negatively supercoiled DNA using an ATP-independent type I mechanism (Dekker et al., 2002).

Several studies have shown that gene position on the chromosome is physiologically significant in bacteria (Bogue et al., 2020; Bryant et al., 2014; Gerganova et al., 2015; Scholz et al., 2019). For example, moving the gene that encodes the nucleoid-associated protein FIS (Factor for Inversion Stimulation) from its native position, proximal to the origin of chromosome replication in *E. coli*, to locations close to the replication terminus, impaired the competitive growth fitness and altered the overarching network regulating DNA topology, resistance to environmental stress, hazardous substances and antibiotics (Gerganova et al., 2015). Among the genes that FIS regulates in *E. coli* (Schneider et al., 1999) and *S.* Typhimurium (Keane & Dorman, 2003) are *gyrA* and *gyrB*.

In *S.* Typhimurium, the *gyrA* and *gyrB* genes are widely separated on the genetic map of the circular chromosome: the *gyrB* gene is located close to the origin of chromosome replication, *oriC*, while *gyrA* is located near to the terminus region, Ter (McClelland et al., 2001). This arrangement closely resembles that seen in the model organism, *E.coli* (Berlyn, 1998; Blattner et al., 1997). It has been proposed that the order of genes along each replichore in the bidirectionally replicated circular chromosome of *E. coli* correlates with the peak levels of expression of genes as a culture passes through each of the major stages of its growth cycle in batch culture (Sobetzko et al., 2012). DNA supercoiling plays an important role in the initiation of chromosome replication, so locating *gyrB* close to *oriC* is consistent with the gene location hypothesis. Bacteria emerging from the lag phase and entering a period of rapid growth in the exponential phase, experience a build-up of negative DNA supercoiling that stimulates the transcription of genes whose products support rapid growth (Colgan et al., 2018; Conter et al., 1997). Rapidly growing bacteria undergo multiple rounds of the initiation of chromosome replication, so genes close to *oriC* are present in more copies per cell than those close to the terminus (Cooper & Helmstetter, 1968). GyrA and GyrB are required in equal amounts to form active DNA gyrase molecules, so the physical separation of *gyrA* from *gyrB* on the chromosome, and their organization as independent transcription units, seem counter-intuitive. In particular, why is *gyrA* so far away from *gyrB* on the circular chromosome of *S.* Typhimurium? The GyrA dimer is a stable structure that lends stability to the tetrameric DNA gyrase (Klostermeier, 2018). Perhaps placing *gyrA* close to the terminus of chromosome replication is well tolerated because a pool of GyrA is present in the cell throughout the growth cycle, available to interact with GyrB produced from the *gyrB* gene close to *oriC*. If this is so, why is this pattern not seen universally in bacteria? This may reflect species-specific differences in gyrase subunit stabilities and in the ways that the GyrA and GyrB subunits interact in different bacteria (Weidlich & Klostermeier, 2020).

The genetically separated pattern of *gyrA* and *gyrB* gene location seen in *S.* Typhimurium and *E. coli* is not found universally among bacteria: many possess a *gyrBA* operon, although none appears to have a *gyrAB* operon. Perhaps this is unsurprising given that the functional domains in eukaryotic type II topoisomerases that are equivalent to the A and B subunits of DNA gyrase are always arranged in the order BA (Berger, 1998; Forterre et al., 2007), suggesting that the ancestor of eukaryotic type II topoisomerases was an operon with a *gyrBA* structure. Examples of other bacteria with a *gyrBA* setup include, *inter alia*, *Listeria monocytogenes* (Glaser et al., 2001), *Mycobacterium tuberculosis* (Unniraman et al., 2002; Unniraman & Nagaraja, 1999), and *Staphylococcus aureus* (Baba et al., 2008). The operon arrangement appears to offer a number of advantages over the individual transcription unit model. Co-expression allows *gyrA* and *gyrB* to share the same promoter and the same transcription regulatory signals. Production of GyrA and GyrB from a common, bicistronic mRNA is likely to facilitate the establishment of equal amounts of each protein. The co-production of GyrA and GyrB might also be expected to enhance the efficiency of gyrase enzyme assembly. It should be noted that the *gyrA* and *gyrB* genes are only seen to be widely separated from one another on the unfolded, circular genetic map of *S.* Typhimurium: the genes may be brought into closer proximity in the folded chromosome within the nucleoid. Furthermore, in the tiny universe of the bacterium's interior, the problem of gyrase assembly from GyrA and GyrB subunits produced from spatially separated mRNA molecules may be an insignificant one (Moffitt et al., 2016). We investigated this issue by building a derivative of *S.* Typhimurium with a *gyrBA* operon and comparing its physiology with that of the wild type.

2 | RESULTS

2.1 | *Constructing a derivative of S.* Typhimurium *with a synthetic* gyrBA *operon*

A kanamycin resistance cassette, *kan*, was inserted adjacent to the *gyrA* gene in *S.* Typhimurium strain SL1344 to serve as a selectable

marker (Experimental procedures). This *gyrA-kan* combination was amplified by PCR, leaving behind the transcription control signals of *gyrA*, and inserted immediately downstream of the *gyrB* gene, creating a *gyrBA* operon with an adjacent *kan* gene that was bordered by directly repeated copies of the FRT sequence; the *kan* gene was then deleted by FLP-mediated site-specific recombination at the *frt* sites. A *kan* gene cassette, flanked by directly repeated *frt* sites, was used to replace the *gyrA* gene at the native *gyrA* location in the *gyrBA*-operon-containing strain; this *kan* cassette was then excised by FLP-mediated recombination. This process produced a derivative of SL1344 that had a *gyrBA* operon at the chromosomal position that is normally occupied by only *gyrB* and had no *gyrA* gene at the chromosomal site where this gene normally resides (Figure 1). The whole-genome sequence of this new strain was determined to ensure that no genetic changes, other than the desired ones, were present; none was detected.

2.2 | *The growth characteristics of the* gyrBA *operon strain*

The growth kinetics of the wild type and the strain with the *gyrBA* operon were compared in batch liquid culture. Cultures grown in Miller's lysogeny broth (LB) (Miller, 1972) had identical growth curves when measured by plating and colony counting or by optical density measurements (Figure S1a,b). Growth was also assessed in a minimal medium in an experiment that included low magnesium stress, an important environmental challenge that *S*. Typhimurium encounters in the macrophage vacuole during infection (Colgan et al., 2018). The wild-type and the *gyrBA*-operon strains were grown in minimal medium *N* (Nelson & Kennedy, 1971) with either 10 μM (low magnesium) or 10 mM (high magnesium) $MgCl_2$. Once again, the two strains had identical growth kinetics (Figure S1c).

2.3 | *Morphology of the strain with the* gyrBA *operon*

The identical growth characteristics of the strain with the *gyrBA* operon and the wild type, both in LB and in minimal medium, showed that producing DNA gyrase from an operon made no difference to the growth cycle and suggested that the cell cycle was unlikely to be altered either. Interference with the timing of major events in the cell cycle (initiation, replication fork passage, and termination) can lead to delays in cell division, resulting in the filamentation of the bacterial cell (Martín et al., 2020; Sharma & Hill, 1995). When we compared the morphologies of mid-exponential-phase cultures of the wild type and the *gyrBA* operon strain by light microscopy, no differences in the shapes of the cells or the frequency of cell filamentation were detected (Figure S2). Taken together with the growth kinetic data, these findings showed that the operonic arrangement of *gyrB* and *gyrA* is well tolerated by *S*. Typhimurium.

2.4 | Sensitivity to gyrase-inhibiting antibiotics

The minimum inhibitory concentrations of gyrase-inhibiting antibiotics were compared for wild-type SL1344 and SL1344 *gyrBA* (Figure 2). Four drugs were tested: coumermycin and novobiocin are coumarins that target the GyrB subunit of DNA gyrase (Lewis et al., 1996), while nalidixic acid and ciprofloxacin are quinolones

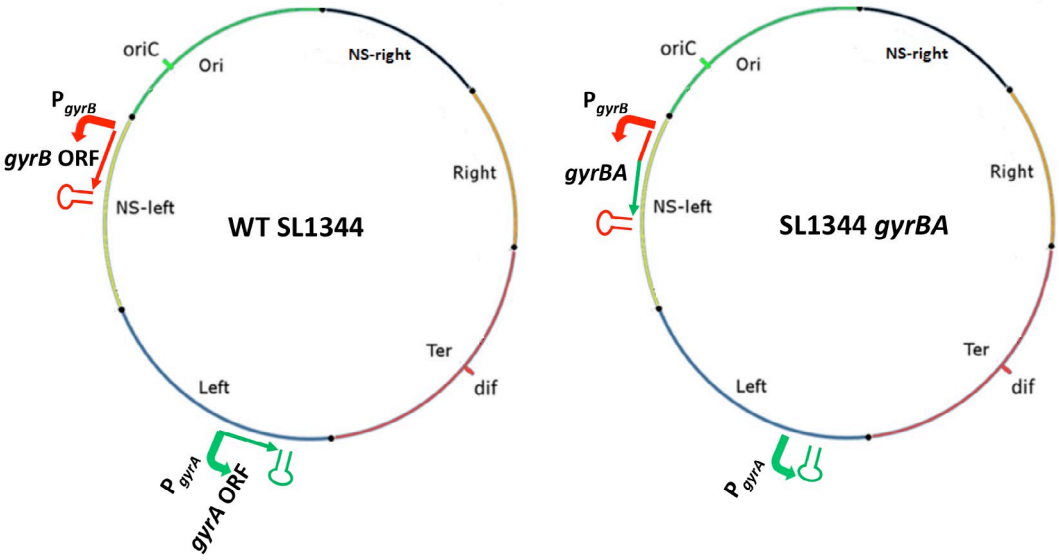

FIGURE 1 Construction of a derivative of *S*.Typhimurium strain SL1344 with a *gyrBA* operon. Chromosomal maps of the WT SL1344 and SL1344 *gyrBA* strains. Positions of *oriC*, *dif*, and chromosome macrodomains are shown. Promoter (angled arrow), protein-coding region (open reading frame, ORF), and the terminator (stem-loop structure) of the genes of interest are shown and color coded. The *gyrA* ORF is green and the *gyrB* promoter and ORF are red. Not to scale [Colour figure can be viewed at wileyonlinelibrary.com]

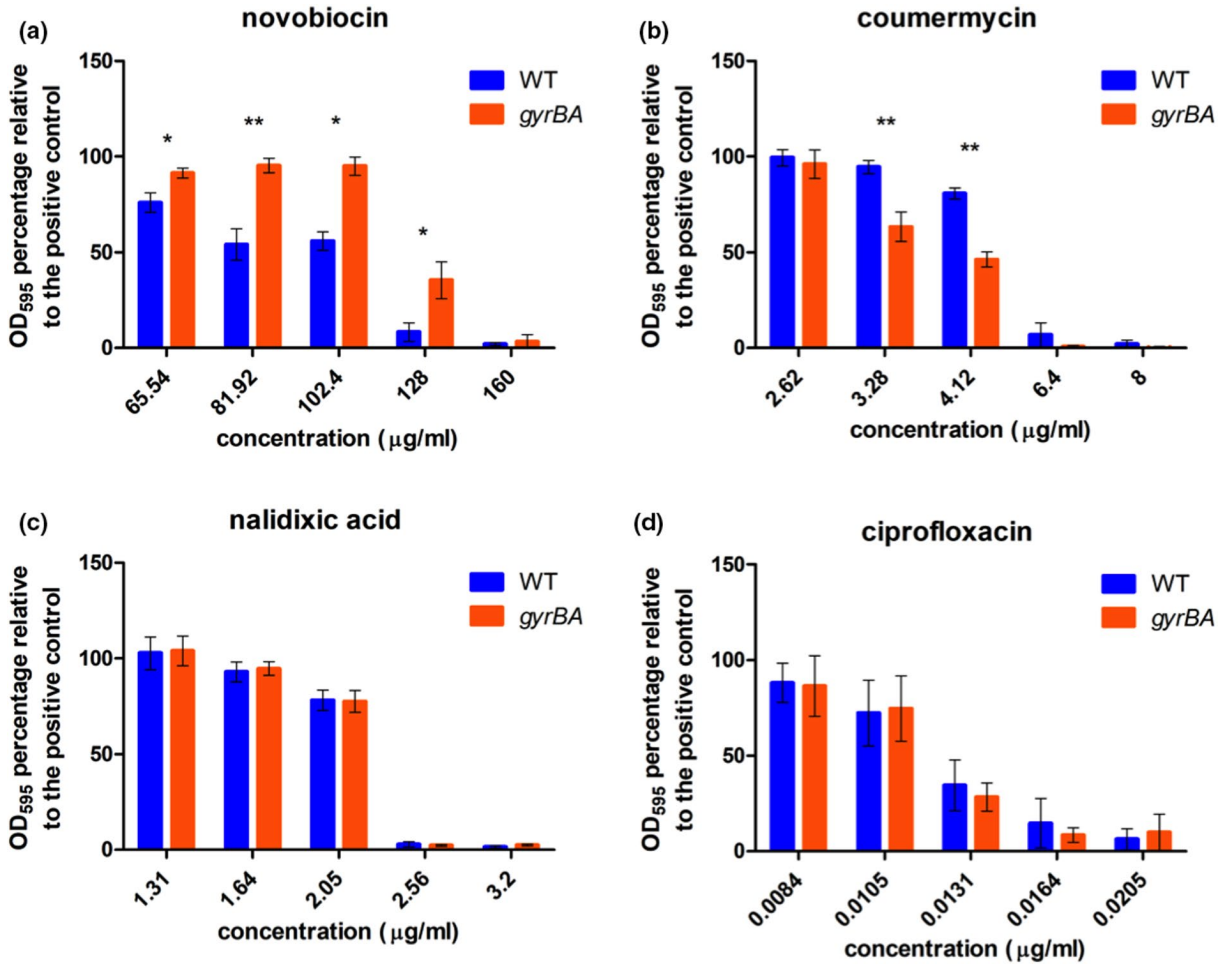

FIGURE 2 Minimum inhibitory concentrations of DNA gyrase-inhibiting antibiotics in the wild-type SL1344 and SL1344 *gyrBA* strains. Cells were grown in a 96-well plate with 1:1.25 serially diluted antibiotics in LB broth for 18 hr at 37°C and aeration. Cell density was measured by OD_{600}. (a) Percentage survival of the WT and SL1344 *gyrBA* in 65.54–160 μg/ml of novobiocin. MIC_{90} of the WT = 128 μg/ml, MIC_{90} of SL1344 *gyrBA* = 160 μg/ml. (b) Percentage survival of the WT and the *gyrBA* in 2.62–8 μg/ml of coumermycin, MIC_{90} = 6.4 μg/ml. (c) Percentage survival of the WT and the *gyrBA* in 1.31–3.2 μg/ml of nalidixic acid, MIC_{90} = 2.56 μg/ml. (D) Percentage survival of the WT and the *gyrBA* in 0.0084–0.0205 μg/ml of ciprofloxacin, MIC_{90} = 0.0164 μg/ml. Error bars represent the standard deviation of at least three biological replicates. Significance was found by unpaired Student's *t*-test, where * = $p < .05$ and ** = $p < .01$ [Colour figure can be viewed at wileyonlinelibrary.com]

that target GyrA (Drlica & Zhao, 1997). Quinolones also target GyrB and coumarins and quinolones inhibit topoisomerase IV, the second type II topoisomerase found in *Salmonella* and related bacteria (Bush et al., 2020). The two strains were equally sensitive to the quinolones, but the SL1344 *gyrBA* strain was more resistant than SL1344 to novobiocin, while SL1344 was more resistant than SL1344 *gyrBA* to coumermycin (Figure 2). The reasons for the differential sensitivity patterns of the strains to the two classes of antibiotics, and for the opposing patterns of resistance to the two coumarins were not determined. Keeping in mind that the coumarins also target topoisomerase IV, we cannot be sure that the differences we observed do not reflect differences in the response of this second drug target in the SL1344 and SL1344 *gyrBA* strain. However, the results indicated that producing the subunits of gyrase from a *gyrBA* operon resulted in coumarin MIC data that were not equivalent to those measured for the strain producing the subunits from physically separate genes.

2.5 | Motility and competitive fitness measurements

The *gyrBA* operon strain was compared with the wild type to assess relative motility on agar plates and competitive fitness in liquid co-culture. The operonic strain showed a small, but statistically significant, reduction in motility compared to the wild type (Figure 3a). The reasons for this were not determined and may reflect changes at one or more levels in the production and operation of the complex motility machinery of the bacterium. In contrast, the two strains were equally competitive when growing in LB (Figure 3b). To perform the competition, the two strains were each marked genetically by insertion on a chloramphenicol resistance (*cat*) cassette that is located in the pseudogene *SL1483*. This *cat* insertion has a neutral effect on fitness and serves simply to allow the competing bacteria to be distinguished by selection on chloramphenicol-containing agar (Lacharme-Lora et al., 2019). The competitions were performed

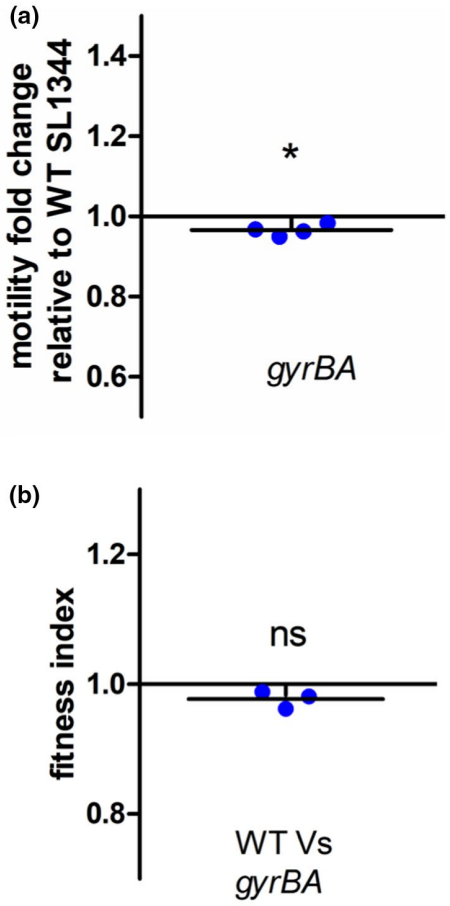

FIGURE 3 Motility and competitive fitness of strain SL1344 *gyrBA*. (a). Diameters of swimming motility were measured after 5 hr incubation at 37°C on soft 0.3% LB agar. The *gyrBA* strain is slightly, but statistically significantly, less motile than the WT. Values below 1 indicate that the strain is less motile than the WT. (b) Fitness of the *gyrBA* strain was compared to the WT SL1344 in LB broth grown for 24 hr with aeration at 37°C. Fitness index (f.i.) = 1 means that the competed strains were equally fit, f.i. < 1 indicates that the competitor strain is less fit than the WT, f.i. > 1 indicates that the competitor is more fit than the WT. The *gyrBA* and the WT were equally fit. Significance was determined by one-sample *T*-test, where $p < .05$ [Colour figure can be viewed at wileyonlinelibrary.com]

between a *cat*-marked wild type and the unmarked *gyrBA* operon strain and separately between a *cat*-marked *gyrBA* operon strain and the unmarked wild type (Figure 3b). No difference in the competitive indices of the two strains was detected in either version of the competition.

2.6 | *Transcription of the separate and the operonic* gyr *genes*

The output of mRNA from the *gyrA* and *gyrB* genes was measured by quantitative PCR in wild-type SL1344 and in SL1344 *gyrBA*, using the transcript of the *hemX* gene as a reference. (Expression of the *hemX* gene does not change under the growth conditions used here

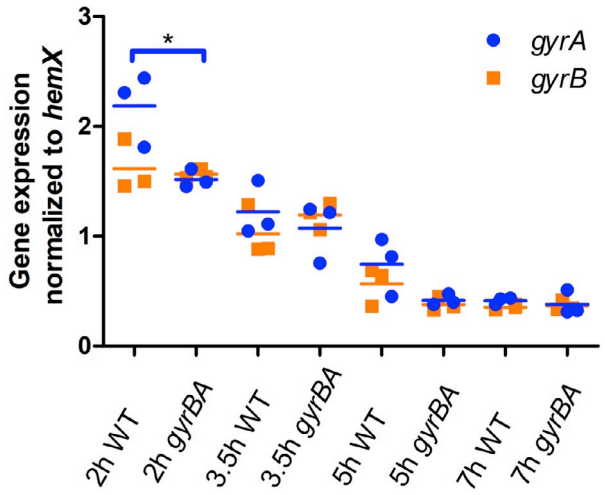

FIGURE 4 Expression of the *gyrA* and *gyrB* genes in wild-type SL1344 (WT) and SL1344 *gyrBA* during growth in liquid culture. Cells were grown in LB broth at 37°C with aeration and samples were taken at 2 hr, 3.5 hr, 5 hr, and 7 hr representing the lag, exponential, exponential-stationary transition, and early stationary phases of growth, respectively. Transcription of *gyrA* and *gyrB* was measured and is reported relative to that of the *hemX* reference gene. Three biological replicates were used. Statistical significance was found by unpaired Student's *T*-test, where $p < .05$ [Colour figure can be viewed at wileyonlinelibrary.com]

[Kröger et al., 2013]). Gyrase gene transcription in both strains was found to vary with the growth cycle stage, with mRNA outputs being highest in the early exponential phase (2-hr time point) and lowest in the stationary phase (Figure 4). In the wild type, the *gyrA* gene (located near Ter, the terminus of chromosome replication) was expressed to a significantly higher level than *gyrB* (located close to *oriC*) at 2 hr. This was interpreted as a reflection of the need to compensate for the effect of increased *gyrB* gene dosage relative to that of *gyrA* in rapidly growing cells (Cooper & Helmstetter, 1968). As the culture approached the stationary phase, the levels of *gyrA* and *gyrB* transcripts equalized, in line with the convergence of *oriC*-proximal and Ter-proximal gene dosages (Figure 4). The formation of the *gyrBA* operon eliminated the difference in *gyrB* and *gyrA* mRNA levels because each became part of the same bicistronic transcript and has adopted the expression profile of *gyrB* (Figure 4).

2.7 | *DNA supercoiling in the strain with a* gyrBA *operon*

The distributions of the topoisomers of the pUC18 reporter plasmid isolated from the wild type and the *gyrBA* operon strain were compared by electrophoresis in a chloroquine-agarose gel (Figure 5). The cultures were grown in LB medium (Figure 5a; S3A) or in minimal medium N with high or low concentrations of $MgCl_2$ (Figure 5b; S3B). In LB, the reporter plasmid was more relaxed in the *gyrBA* strain than in the wild type (Figures 5a, S3b). Low-magnesium growth was used to mimic one of the stresses experienced by *Salmonella* in the macrophage vacuole. In the high $MgCl_2$ control, the wild type and

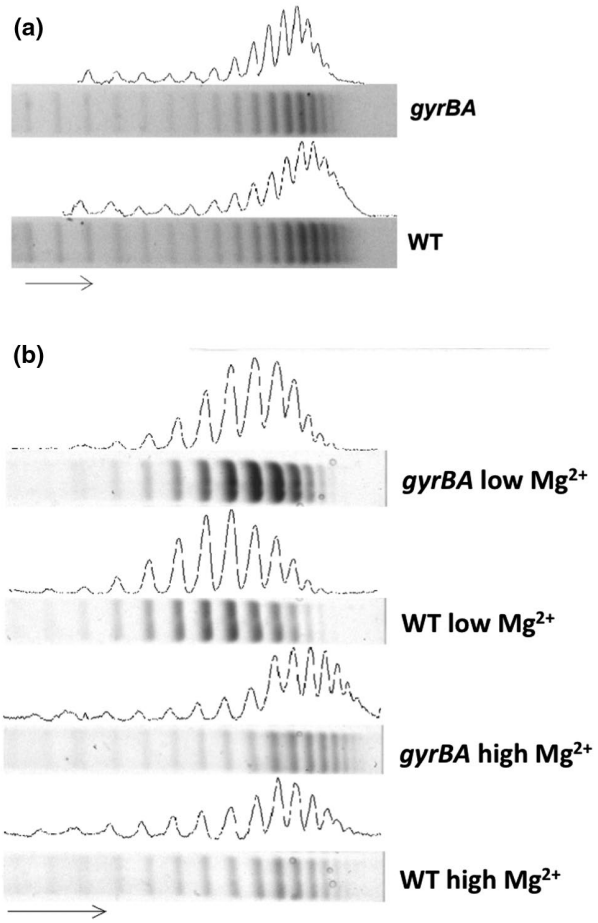

FIGURE 5 Reporter plasmid DNA supercoiling in SL1344 *gyrBA*. The pUC18 reporter plasmid was extracted from the WT and the SL1344 *gyrBA* strains at the stationary phase of growth and electrophoresed on a 0.8% agarose gel containing 2.5 μg/ml of chloroquine. The arrow shows the direction of migration, with the more supercoiled plasmid topoisomers at the right of the gel. (a). Global DNA supercoiling pattern of the WT and the *gyrBA* strain when grown in LB. (b). Global DNA supercoiling pattern of the WT and the *gyrBA* strain when grown in minimal medium N with high (10 mM) $MgCl_2$ or low (10 μM) $MgCl_2$. Sample lanes are supplemented with densitometry profiles that were generated with ImageJ. The analysis is representative of four biological replicates

the *gyrBA* operon strain differed in their reporter plasmid distributions: DNA from the *gyrBA* strain was more negatively supercoiled than that from the wild type and showed a linking number difference (ΔLk) of −3 (Figures 5b, S3b). At the low $MgCl_2$ concentration, the topoisomer distributions were more relaxed in both strains than in the high $MgCl_2$ controls (ΔLk = +3). The reporter plasmid from the *gyrBA* operon strain was also more negatively supercoiled than that from the wild type, with the peak in its topoisomer distribution being approximately two linking numbers below that of the wild type (Figures 5b, S3b).

DNA relaxation occurs in *Salmonella* cells as they adjust to the macrophage vacuole; this forms part of the activation mechanism for the genes in the SPI-2 pathogenicity island (Cameron & Dorman, 2012; O Cróinín et al., 2006; Quinn et al., 2014). The products of these virulence genes protect the bacterium by inhibiting the fusion of the vacuole with lysosomes (Garvis et al., 2001). We, therefore, monitored SPI-2 gene transcription in our two strains.

2.8 | SPI-1 and SPI-2 gene expression in the gyrba operon strain

The SPI-1 and SPI-2 pathogenicity islands encode distinct type 3 secretion systems and effector proteins that are used to invade epithelial cells (SPI-1) or to survive in the intracellular vacuole (SPI-2) (Figueira & Holden, 2012; van der Heijden & Finlay, 2012; Hensel, 2000). Transcription of SPI-1 genes was monitored using a gfp^+ reporter fusion under the control of the *prgH* promoter, P_{prgH}, while a gfp^+ fusion to the *ssaG* promoter (P_{ssaG}) was used to monitor SPI-2 gene transcription. Wild type and *gyrBA* operon strains harboring these fusions were grown in LB medium (Figure 6a, b) or in minimal medium N, supplemented with high or low concentrations of $MgCl_2$. (Figure 6c-f). The cultures were grown with aeration at 37°C in 96-well plates, and green fluorescence was measured throughout the growth cycle. The results obtained showed that in LB medium and in minimal medium N, SPI-1 transcription was indistinguishable between the wild type and the *gyrBA* operon strains (Figure 6a, c, e). SPI-2 transcription was equivalent in both strains growing in LB (Figure 6b) or in a minimal medium with high $MgCl_2$ (Figure 6d). However, SPI-2 transcription occurred at reduced levels in the *gyrBA* strain in the later stages of the growth cycle under low magnesium conditions (7.8% lower between 800- and 1460-min time points in Figure 6f). These findings showed that when the subunits of gyrase are produced from an operon, rather than from separate *gyrA* and *gyrB* genes in their native chromosome locations, the normal expression profile of the SPI-2 virulence gene cluster is disrupted, but that this is conditional on growth in a low magnesium medium.

2.9 | *Impact of the gyrase operon on cell infection by* Salmonella

The abilities of the wild type and the *gyrBA* operon strains to invade and to replicate in cultured mammalian cells were compared. Bacteria, grown to the mid-exponential phase to promote SPI-1 gene expression, were used to infect RAW264.7 macrophage. When intracellular bacteria were then enumerated post-invasion, fewer of the *gyrBA* operon strain cells were detected than wild-type cells at and after the 16-hr time point (Figure 7). This reduction in bacterial survival correlated with the diminished SPI-2 expression detected in the *gyrBA* operon strain in low Mg^{2+}, a macrophage relevant condition.

3 | DISCUSSION

The genes in *Salmonella* that encode DNA gyrase, *gyrA*, and *gyrB*, are located at the opposite ends of the left replichore of the

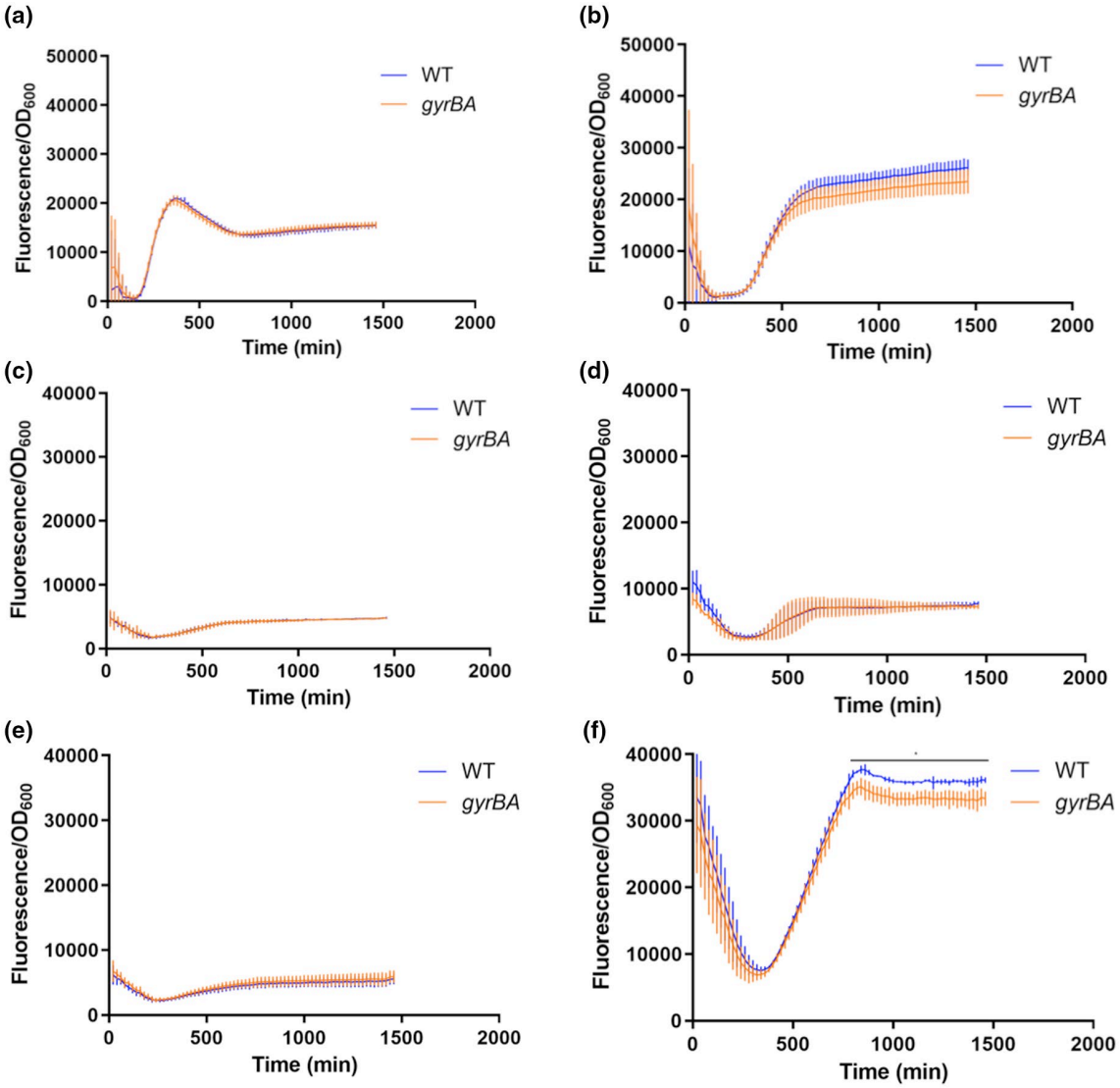

FIGURE 6 Expression of genes in the SPI-1 and SPI-2 pathogenicity islands in wild-type SL1344 (WT) and SL1344 *gyrBA*. Expression of *gfp*$^{+}$ reporter gene fusions was measured in the wild-type and SL1344 *gyrBA* strains every 20 min over a 24-hr. period. (a). SPI-1 expression in the *gyrBA* strain was identical to that in the WT in LB. (b). SPI-2 expression in the *gyrBA* strain was identical to that of the WT in LB. (c). SPI-1 expression in minimal medium N with high $MgCl_2$ concentration (10 mM) was repressed in both the WT and the *gyrBA* strain. (d). SPI-2 expression in minimal medium N with high $MgCl_2$ concentration was repressed in both the WT and the *gyrBA* strains. (e). SPI-1 expression in minimal medium N with a low $MgCl_2$ concentration (10 μM) was repressed in both the WT and the *gyrBA* strains. (F) SPI-2 expression in minimal medium N with low $MgCl_2$ concentration was lower in the *gyrBA* strain than in the WT at the stationary phase of growth. All plots are the results of at least three biological replicates; error bars represent the standard deviation. Statistical significance was found by Student's unpaired *T*-test, where $p < .05$ [Colour figure can be viewed at wileyonlinelibrary.com]

chromosome (Figure 1). In contrast, many other bacteria, such as *Listeria monocytogenes*, *Staphylococcus aureus*, and *Mycobacterium tuberculosis*, possess a *gyrBA* operon (Baba et al., 2008; Glaser et al., 2001; Unniraman et al., 2002; Unniraman & Nagaraja, 1999). As a first step in assessing the significance of the stand-alone gyrase gene arrangement versus the operon model, we constructed a derivative of *S*. Typhimurium with a *gyrBA* operon at the chromosomal location that is normally occupied by *gyrB* alone, while removing the individual *gyrA* gene from its native position in the genome. This strain, with the *gyrB* and *gyrA* genes transcribed from a common promoter (P_{gyrB}) and located close to the origin of chromosomal replication, had normal growth characteristics (Figure S1) and cell morphology (Figure S2).

Although the production of DNA gyrase from an operon was well tolerated by *S*. Typhimurium, the operon strain differed from the wild type in a number of phenotypic characteristics. These included a modest decrease in competitive fitness in the operon strain (Figure 3) that hinted at generalized impacts on physiology. There were subtle differences in sensitivities to coumarin antibiotics, but not quinolones, that distinguished the operon strain from the wild type (Figure 2). In *E. coli*, the *gyrA* and *gyrB* genes respond differently to treatment with DNA gyrase inhibitors: while coumarins and

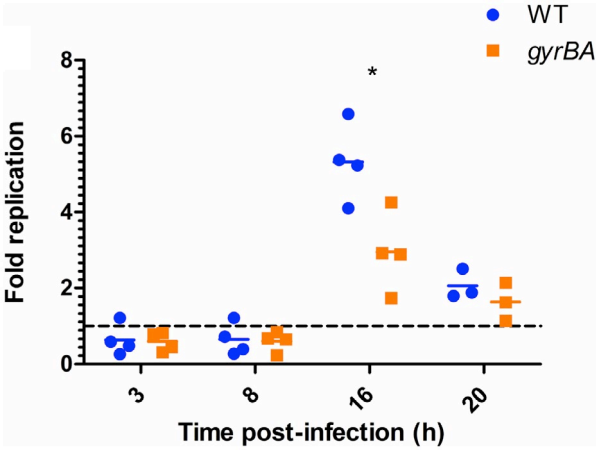

FIGURE 7 SPI-1-mediated entry and survival of the WT and SL1344 *gyrBA* strain in cultured RAW264.7 macrophage cells. Cells were infected with SPI-1-induced bacteria, grown to mid-exponential phase to promote SPI-1-mediated invasion. Survival and replication were measured by enumerating colony-forming units (CFUs) at 3 hr, 8 hr, 16 hr, and 20 hr post-infection. Fold replication represents the number of CFUs recovered at a particular time point divided by the CFU number at 1 hr. Mean and individual replicates are shown. Significance at 16 hr was found by unpaired Student's *T*-test, where $p < .05$ [Colour figure can be viewed at wileyonlinelibrary.com]

quinolones both increase the expression of *gyrA*, the expression of only *gyrB* is induced by coumarins (Neumann & Quiñones, 1997). In our operon strain, the coumarin-sensitive *gyrB* promoter drives the transcription of both *gyrB* and *gyrA*, and this may have contributed to the difference between the operon strain and the wild type in responding to the coumarin challenge. It is also possible that the differences in coumarin sensitivity may have involved indirect effects of operonic gyrase production on processes involved in drug uptake and/or be due to differential effects on the activity of the bacterium's second coumarin target, topoisomerase IV, in the wild type and gyrase operon strains.

The stand-alone *gyrA* gene is expressed to a higher level than *gyrB* in the wild type, albeit from a distant location on the chromosome (Figure 4). Also, the stable GyrA protein seems to play a foundational role in the assembly of DNA gyrase (Klostermeier, 2018; Weidlich & Klostermeier, 2020). Placing the *gyrA* gene under the control of the P_{gyrB} promoter in the *gyrBA* operon equalized the levels of the transcripts from the two genes (Figure 4) by making them parts of a bicistronic operon (Figure 1). Operon formation, with the associated equalizing of *gyrB* and *gyrA* transcript levels, may have altered the cellular ratio of GyrB and GyrA, as well as their site of production, in ways that produced the effects we have detected on DNA topology, coumarin sensitivity, SPI-2 expression, and *Salmonella* virulence.

The expression of the horizontally acquired SPI-2 pathogenicity island allows *S*. Typhimurium, a facultative intracellular pathogen, to survive in the hostile environment of the macrophage vacuole. The *gyrBA* operon strain both expressed SPI-2 less well (Figure 6) and survived less well than the wild type in the macrophage (Figure 7). The *Salmonella*-containing vacuole of the macrophage is a stressful, low magnesium environment where the SPI-2-encoded type 3 secretion system and its associated effector proteins, play a key protective role (Figueira & Holden, 2012; van der Heijden & Finlay, 2012; Hensel, 2000). DNA relaxation contributes to the full expression of SPI-2 genes (Cameron & Dorman, 2012; Quinn et al., 2014) and DNA in *S*. Typhimurium becomes relaxed when the bacterium is in the macrophage (O Cróinín et al., 2006), The *gyrBA* operon strain maintained its DNA in a less relaxed state in a low-magnesium environment (Figure 5) and this may explain the poorer transcription of SPI-2 that was seen in low magnesium growth (Figure 6).

Our data reveal a distinction between the sensitivity of genes encoding housekeeping functions and genes in the horizontally acquired accessory genome to the production of DNA gyrase from an operon. Genes that have been acquired by *Salmonella* via horizontal gene transfer (HGT) are more A + T-rich than core genome members and are subject to multifactorial control that includes a prominent role for nucleoid-associated proteins such as H-NS, FIS, IHF, and HU (Banda et al., 2019; Cameron & Dorman, 2012; Dillon & Dorman, 2010; Fass & Groisman, 2009; Mangan et al., 2006, 2011; Quinn et al., 2014). These genes also display sensitivity to changes in DNA topology (Cameron & Dorman, 2012; O Cróinín et al., 2006; Quinn et al., 2014). SPI-2 expression is held in check in *Salmonella* until it is required during adaptation to the macrophage vacuole and a shift in global DNA supercoiling levels is a component of the activation signal (Cameron & Dorman, 2012; O Cróinín et al., 2006; Quinn et al., 2014). The shift in global DNA supercoiling values that we see in *Salmonella*, growing in a minimal medium that mimics the intravacuolar environment, dysregulates SPI-2 transcription and compromises *Salmonella* infectivity. This finding is consistent with proposals that *Salmonella* maintains a level of DNA topology that is optimized to control the activities, and the expression, of mobile genetic elements that include pathogenicity islands, bacteriophage, and transposons (Cameron et al., 2011; Champion & Higgins, 2007; Higgins, 2016).

We have shown experimentally that there is no absolute barrier to the organization of the *gyrB* and *gyrA* genes as a *gyrBA* operon in *Salmonella*. Furthermore, there are many examples of naturally occurring *gyrBA* operons among bacterial species. Why is this arrangement not found universally? Sharing a common promoter, common transcriptional regulatory features, and a common chromosomal location would appear to offer the advantages of coordinated gene expression (Price et al., 2005) and physical co-production of protein products that will need to combine with a fixed stoichiometry to form an active product (Dandekar et al., 1998; Pal & Hurst, 2004; Swain, 2004). Indeed, the coupling of transcription and translation in prokaryotes may aid the production of operon-encoded proteins that are required in stoichiometric amounts (Li et al., 2014; Rocha, 2008). Often, but not invariably, operons are composed of genes that contribute to a common pathway (de Daruvar et al., 2002; Lawrence & Roth, 1996; Price et al., 2006; Rogozin et al., 2002) and that is true of the *gyrBA* operon. Colocation of genes within an operon facilitates their collective translocation via horizontal gene transfer, allowing them to replace lost or mutated copies in the recipient cell (Lawrence

& Roth, 1996). According to this "selfish operon" hypothesis, this creates selective pressure for the maintenance of an operon structure. However, since the loss of either *gyrA* or *gyrB* is lethal, the gyrase operon may be one of the exceptions to the selfish operon rule, because gyrase-deficient recipients cannot exist.

We conducted a survey of gyrase gene locations in bacteria to assess the frequency of the stand-alone arrangement seen in *Salmonella* and the *gyrBA* operon arrangement seen in other species (Experimental procedures). We were unable to find any example of a bacterium with a *gyrAB* operon. It should be noted that the functional domains corresponding to GyrA and GyrB in eukaryotic type II topoisomerases are found in the order BA (Berger, 1998; Forterre et al., 2007), suggesting that their ancestor may have been encoded by an operon with a *gyrBA* structure. The results of the survey are shown in Table 1, where bacteria are grouped according to their gyrase gene arrangement, using *oriC* as a reference point. Figure 8 shows a phylogenetic tree summarizing the occurrence of different gyrase gene arrangements among bacteria from the four groups listed in Table 1.

Inversions of DNA between the left and the right replichores were seen frequently and these followed no obvious patterns. This is in agreement with a previous finding that, while the distance to the origin is highly conserved, inversions of genes around the Ter region of a chromosome are frequent and well tolerated in *E. coli* and *Salmonella* (Alokam et al., 2002). Various relative arrangements of *gyrA* and *gyrB* were observed and subdivided into four groups: Group 1 had *gyrB* and *gyrA* positioned separately, with *gyrB* near *oriC*; Group 2 had *gyrB* and *gyrA* positioned separately, with the position of *gyrB* being variable; Group 3 had *gyrB* and *gyrA* arranged as a *gyrBA* operon in the immediate vicinity of *oriC*; Group 4 had *gyrB* and *gyrA* arranged as a *gyrBA* operon at a distance from *oriC*. The arrangements of *gyrA* and *gyrB* genes were categorized into the four Groups not only according to the relative positions of *gyrA* and *gyrB*, but also according to the degree of the conservation of the genetic environment of *gyrB*.

Table 1 suggests that all members of the class gammaproteobacteria (phylum Proteobacteria), including *E. coli* and *Salmonella*, some alpha-proteobacteria, beta-proteobacteria, and epsilon-proteobacteria are in Group 1. Group 2 contains some alpha-, beta- and delta-proteobacteria, members of the family *Streptococcaceae* (order Lactobacillales, phylum Firmicutes); members of the class Flavobacteriia; multiple members of the phylum Bacteroidetes; Acidobacteria and *Deinococcus radiodurans*. Group 3 was composed of members of the phylum Actinobacteria, classes Clostridia and Bacilli (phylum Firmicutes), family *Enterococcaceae* and family *Lactobacillaceae* (order Lactobacillales, phylum Firmicutes) order Fusobacteria (phylum Fusobacteria) and phylum Tenericutes. Finally, Group 4 consisted of members of the phylum Chlamydiae. There is perhaps more variation within Group 4, but this was not detected using the method employed here. *Mycoplasma* is an anomaly of Group 3, since not all its species clearly belong to this group. Some *Mycoplasma* possess the expected conserved genes 5' to *gyrB*, but not in its immediate vicinity. However, the orientation of genes 5' to *gyrB* remains favorable for the initiation of its transcription, therefore, *Mycoplasma* is placed in Group 3. It was clear from the analysis that members of the same taxonomic rank do not necessarily have to belong to the same Group, especially in diverse phyla. For example, both Group 2 and Group 3 arrangements are present within the Firmicutes. Moreover, both arrangements are present within the order Lactobacillales alone. Some less diverse phyla such as Fusobacteria and Chlamydiae belong to only one Group. No variation was found within families.

It was difficult to determine whether given taxons were enriched in particular groups in Table 1, so a phylogenetic tree was plotted that included all of the bacteria in the table (Figure 8). The tree was constructed using the phylogenetic tree generator phyloT, based on NCBI taxonomy (Letunic & Bork, 2019) and the positions of the branches were manually reviewed with the aid of the NCBI taxonomy browser. It is apparent that one Group can be present in multiple unrelated phyla and that one phylum can contain members of several Groups, illustrating a high level of diversity of *gyrA* and *gyrB* chromosomal arrangements. However, certain patterns are discernable. Bacteria from Group 1 are exclusively located in phylum Proteobacteria. All the members of phylum Bacteroidetes that were investigated belong to Group 2, but other phyla can also contain some members of Group 2. The Group 3 arrangement occurs with high frequency in the superphylum Terrabacteria (Firmicutes, Tenericutes, Actinobacteria, Deinococcus), although this arrangement can be encountered elsewhere too. Finally, all of the tree members of Group 4 shown belong to the phylum Chlamydiae. No other phylum was found to contain bacteria of Group 4, but the existence of the Group 4 arrangement outside of the Chlamydiae cannot be ruled out. It is also difficult to draw clear parallels between the lifestyle of an organism and the Group to which it belongs, since bacteria of various lifestyles can be members of the same Group. The analysis presented here is indicative rather than exhaustive: it is possible that further sampling will broaden the existing Groups and reveal further details.

When the immediate genetic environment of both genes in bacteria listed in Table 1 was studied, one distinct pattern was found—homologs of *dnaA* (encoding chromosomal replication initiation protein DnaA), *dnaN* (encoding the beta subunit of DNA polymerase III), and *recF* (encoding the DNA repair protein RecF) or at least one of these three genes, are found directly upstream of *gyrB* gene in all bacteria in which *gyrB* is located in the immediate vicinity of *oriC*, such as most bacteria of Groups 1 and 3 (Table 1). Transcription from these co-oriented neighboring genes provides a strong input of DNA relaxation (Sobetzko, 2016) that stimulates the transcription of the supercoiling-sensitive *gyrB* promoter, P_{gyrB} (Menzel & Gellert, 1987). This is true of most bacteria where *gyrB* is in the immediate vicinity of *oriC* and *gyrA* is located either about 20% of the chromosome further away or is a part of a *gyrBA* operon. Bacteria with a *gyrBA* operon that is not in the immediate vicinity of *oriC* (such as *Chlamydia psittaci*) and bacteria with the two *gyr* genes separated by about 20% of the chromosome, such as *Myxococcus xanthus* (together with

TABLE 1 Relative positions of *gyrB* and *gyrA* across bacterial species

Organism (phylum, lowest clade sharing the arrangement)	*gyrB* to *oriC* distance in bp, Left or Right replichore	*gyrB* to *oriC* distance as % total chromosome (%)	*gyrA* to *oriC* distance in bp, Left or Right replichore*	*gyrA* to *oriC* distance as % total chromosome (%)
Group 1 (*gyrB* and *gyrA* positioned separately, *gyrB* near *oriC*)				
Escherichia coli	45,409, Right	0.98	1,585,679, Right	34.20
Salmonella enterica serovar Typhimurium	42,033, Left	0.86	1,730,509, Left	35.48
Salmonella enterica serovar Gallinarum	37,634, Right	0.81	1,382,662, Left	29.68
Shigella flexneri	57,368, Left	1.25	1,577,518, Left	34.24
Yersinia pestis	37,176, Left	0.79	1,073,028, Right	22.82
Vibrio cholerae	10,386, Right	0.35	1,329,436, Right	44.90
Pseudomonas aeruginosa	2,248, Right	0.04	2,708,909, Left	43.26
Xanthomonas axonopodis (all above are Proteobacteria, class Gammaproteobacteria)	3,161, Right	0.06	1,876,940, Right	36.27
Azospirillum sp. (Proteobacteria (α), order Rhodospirillales)	179,561, Left	5.42	1,595,259, Right	48.17
Caulobacter crescentus (Proteobacteria (α), order Caulobacterales)	166,112, Right	4.14	1,744,542, Right	43.43
Azoarcus sp. (Proteobacteria (β), order Rhodocyclales)	32,299, Right	0.61	1,182,414, Left	22.49
Burkholderia cepacia (Proteobacteria (β), Burkholderiales)	160,154, Right	4.62	859,834, Left	24.82
Campylobacter jejuni (Proteobacteria, class Epsilonproteobacteria)	635, Right	0.04	653,170, Left	40.12
Group 2 (*gyrB* and *gyrA* positioned separately, *gyrB* position variable)				
Myxococcus xanthus (Proteobacteria (Δ), order Myxococcales)	310,304, Right	3.40	872,133, Right	9.54
Bacteroides thetaiotaomicron (Bacteroidetes, family *Bacteroidaceae*)	246,107, Right	3.93	2,199,265, Left	35.10
Bacteroides fragilis (Bacteroidetes, family *Bacteroidaceae*)	155,636, Right	2.99	2,420,574, Left	46.50
Rickettsia prowazekii (Proteobacteria (α), order Rickettsiales)	382,412, Left	34.40	250,129, Right	22.50
Neisseria gonorrhoeae (Proteobacteria (β), order Neisseriales)	412,632, Left	19.16	616,174, Right	28.61
Streptococcus pneumoniae (Firmicutes, family *Streptococcaceae*)	786,742, Left	37.25	951,471, Right	45.05
Streptococcus pyogenes (Firmicutes, family *Streptococcaceae*)	521,569, Left	27.53	897,992, Right	47.40
Flavobacterium columnare (Bacteroidetes, class Flavobacteria)	448,681, Left	14.19	1,240,595, Right	39.22
Prevotella intermedia (Bacteroidetes, family *Prevotellaceae)*	267,997, Left	12.64	697,114, Right	32.89
Sphingobacterium sp. (Bacteroidetes, class Sphingobacteriia)	2,928,149, Right	47.03	2,182,864, Left	35.06
Porphyromonas gingivalis (Bacteroidetes, family *Porphyromonadaceae)*	552,805, Left	23.59	873,251, Left	37.26
Deinococcus radiodurans (Deinococcus-Thermus, class Deinococci)	911,819, Right	34.45	714,641, Left	26.88
Acidobacterium capsulatum (Acidobacteria, class Acidobacteria)	685,949, Right	16.62	33,951, Left	0.82
Group 3 (*gyrBA* operon near *oriC*)				
Geobacter sulfurreducens (Proteobacteria (Δ), order Desulfuromonadales)	1831, Right	0.05	Downstream of *gyrB*	
Pelobacter carbinolicus (Proteobacteria (Δ), order Desulfuromonadales)	2057, Right	0.06	downstream of *gyrB*	

(Continues)

TABLE 1 (Continued)

Organism (phylum, lowest clade sharing the arrangement)	*gyrB* to *oriC* distance in bp, Left or Right replichore	*gyrB* to *oriC* distance as % total chromosome (%)	*gyrA* to *oriC* distance in bp, Left or Right replichore*	*gyrA* to *oriC* distance as % total chromosome (%)
Streptomyces coelicolor (Actinobacteria, class Actinobacteria)	3,994, Left	0.05	downstream of *gyrB*	
Mycobacterium tuberculosis (Actinobacteria, class Actinobacteria)	2,643, Right	0.06	downstream of *gyrB*	
Micrococcus luteus (Actinobacteria, family *Micrococcaceae*)	2,843, Right	0.11	downstream of *gyrB*	
Clostridium tetani (Firmicutes, class Clostridia)	2,472, Left	0.09	downstream of *gyrB*	
Lactobacillus brevis (Firmicutes, family *Lactobacillaceae*)	2,557, Right	0.11	downstream of *gyrB*	
Enterococcus faecalis (Firmicutes, family *Enterococcaceae*)	5,883, Right	0.20	downstream of *gyrB*	
Listeria monocytogenes (Firmicutes, order Bacillales)	3,776, Right	0.13	downstream of *gyrB*	
Bacillus subtilis (Firmicutes, order Bacillales)	2,546, Right	0.06	downstream of *gyrB*	
Spirochaeta thermophila (Spirochaetes, class Spirochaetia)	941, Left	0.38	downstream of *gyrB*	
Fusobacterium nucleatum (Fusobacteria, class Fusobacteria)	3,170, Left	0.15	downstream of *gyrB*	
Borrelia burgdorferi (*Spirochaetes*, class Spirochaetia)	1,268, Left	0.14	downstream of *gyrB*	
Mycoplasma haemofelis (Tenericutes, class Mollicutes)	33,798, Right	2.94	downstream of *gyrB*	
Group 4 (*gyrBA* operon distant from *oriC*)				
Chlamydia psittaci (Chlamydiae, class Chlamydia)	573,957, Left	48.97	downstream of *gyrB*	
Chlamydia trachomatis (Chlamydiae, class Chlamydia)	504,740, Left	48.42	downstream of *gyrB*	
Waddlia chondrophila (Chlamydiae, class Chlamydia)	1,044,601, Right	49.36	downstream of *gyrB*	

*Where *gyrB* and *gyrA* form an operon, *gyrA* is universally located downstream of *gyrB*.

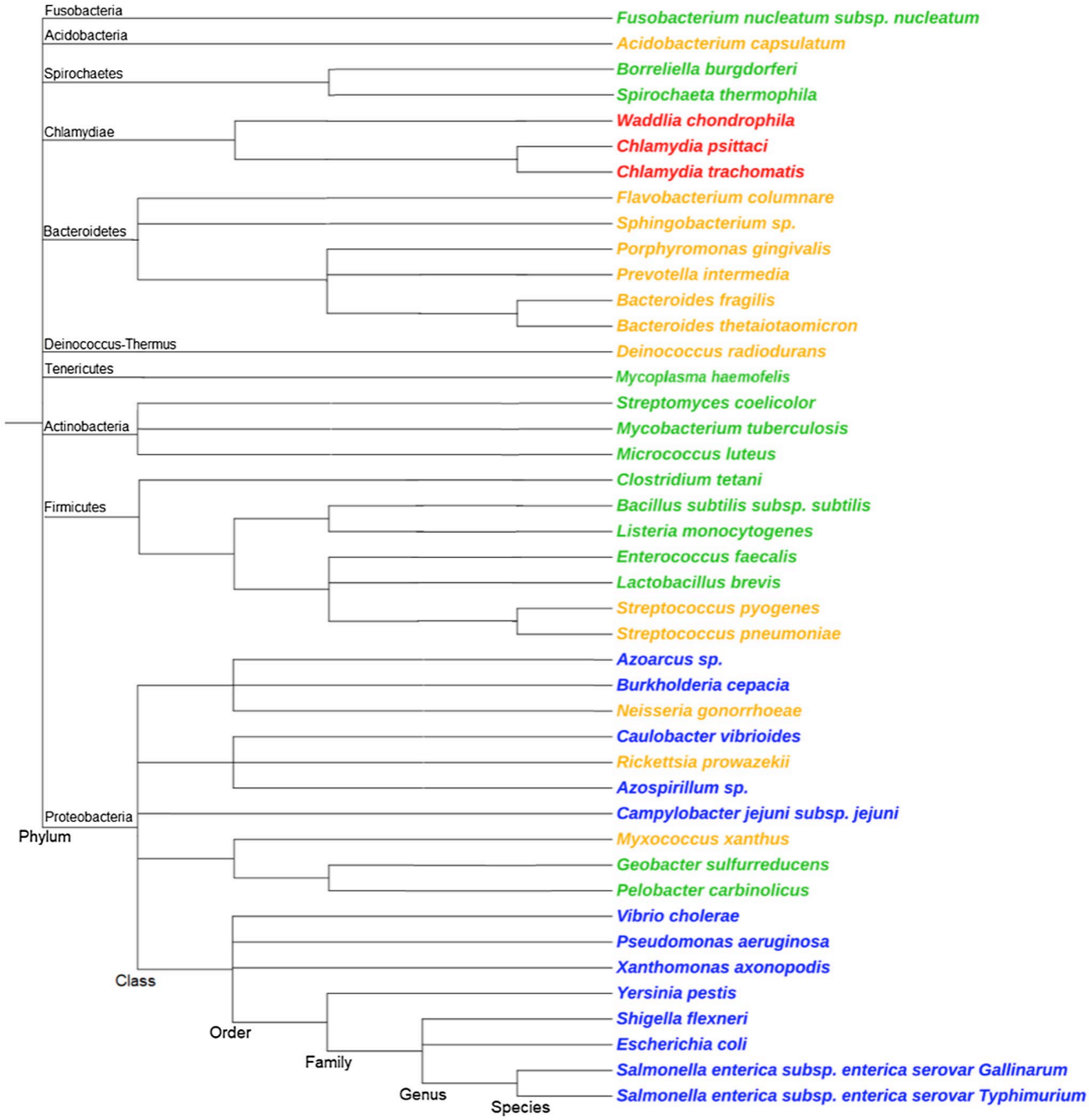

FIGURE 8 Phylogenetic tree of bacteria that belong to different groups based on their *gyrA* and *gyrB* arrangement. The phylogenetic tree was built in phyloT, a phylogenetic tree generator based on NCBI taxonomy (Letunic & Bork, 2019). Each of the four groups (see Table 1) of *gyrA* and *gyrB* arrangements is indicated by color. Group 1, blue: *gyrA* and *gyrB* are at separate locations, with a conserved genetic environment 5' to *gyrB*. Group 2, orange: *gyrA* and *gyrB* are at separate locations, with a non-conserved genetic environment 5' to *gyrB*. Group 3, green: *gyrBA* operon, conserved genetic environment 5' to *gyrB*. Group 4, red: *gyrBA* operon, non-conserved genetic environment 5' to *gyrB*. Phyla names are indicated [Colour figure can be viewed at wileyonlinelibrary.com]

some Bacteroidetes) that satisfy the gene positional parameters characteristic of Group 1, possess *gyrB* with a non-conserved genetic neighborhood. Bacteria of Groups 2 and 4 do not have a conserved genetic environment around *gyrB*. The conservation of the genetic neighborhood 5' to *gyrB* seems to be more important than the subjective proximity to *oriC*. Therefore, genetic neighborhood conservation was used as a parameter to decide the groupings in Table 1. The frequent association of *gyrB* with the *dnaA*, *dnaN*, and *recF* genes; the higher conservation of *gyrB*'s position in comparison to *gyrA*; the transcriptional response of *gyrB* to quinolones—all indicate that the conservation of the physical location of *gyrB*, but not *gyrA*, is essential in many bacteria. These findings reveal important information about chromosome composition in natural bacteria and can help guide attempts at synthetic chromosome design.

4 | EXPERIMENTAL PROCEDURES

4.1 | Bacterial strains and culture conditions

The bacterial strains used in this study were the derivatives of *S*. Typhimurium strain SL1344 and their details are listed in Table 2. Bacterial cultures were grown routinely either in Miller's lysogeny broth (LB) (Miller, 1972) or in minimal medium N (Nelson & Kennedy, 1971). Bacteriophage P22 HT 105/1 *int*-201 was used for generalized transduction during strain construction (Schmieger, 1972). Phage lysates were filter-sterilized and stored at 4°C in the dark. Bacterial strains were stored as 35% glycerol stocks at −80°C and freshly streaked on agar plates for each biological replicate. Four milliliters of LB broth were inoculated with a single colony and grown for 18 hr. This overnight culture was sub-cultured into fresh 25 ml of LB broth normalizing to an OD_{600} of 0.003, unless otherwise stated, and grown to the required growth phase. The standard growth conditions for all bacterial strains were 37°C, 200 rpm, unless otherwise stated. For culturing in minimal medium, overnight cultures were prepared as described above. One milliliter of overnight culture was washed three times with a minimal medium N of the required $MgCl_2$ concentration to remove nutrients, sub-cultured into minimal medium of the corresponding $MgCl_2$ concentration in a total volume of 25 ml and grown for 24 hr to pre-condition the bacteria. The pre-conditioned culture was sub-cultured into 25 ml of fresh minimal medium N adjusted to an OD_{600} of 0.03 and grown for a further 24 hr to obtain a culture in the stationary phase of growth.

To measure growth characteristics of a bacterial culture, an overnight culture was adjusted to an OD_{600} of 0.003 in 25 ml of fresh LB broth and grown at the standard conditions for 24 hr in the appropriate liquid medium. The optical density of the culture at OD_{600} was measured at 1-hr intervals for the first 3 hr and then every 30 min until 8 hr; the last reading was taken at 24 hr. Measurements were taken using a Thermo Scientific BioMate 3S spectrophotometer with liquid cultures in plastic cuvettes. To measure the growth characteristics of bacterial culture in the minimal medium with altered Mg^{2+} concentration, an overnight bacterial culture was washed in the minimal medium with an appropriate concentration of $MgCl_2$ and pre-conditioned for 24 hr. The pre-conditioned culture was adjusted to an OD_{600} of 0.03 in 25 ml of fresh medium in two flasks and the OD_{600} was measured every hour beginning from 2 hr post-time zero to 8 hr. Separate cultures were set up similarly to measure OD_{600} every hour from 8 hr to 15 hr. In this way, the number of times each flask was opened and sampled was minimized to yield reliable and reproducible measurements.

The growth characteristics of bacterial cultures in LB broth were also measured by viable counts. The culture was grown in the same way as for spectrophotometry, and an aliquot was taken at 2 hr, 4 hr, 6 hr, 8 hr, and 24 hr, serially diluted and spread on LB agar plates to give between 30 and 300 colonies after overnight incubation at 37°C. The bacterial colony counts were expressed as colony-forming units per milliliter (cfu/ml).

TABLE 2 Bacterial strains

Strain name	Genotype/Description	Source/reference
SL1344	*rpsL hisG*	Hoiseth and Stocker (1981)
SL1344 *gyrA*::*kan*	Kanamycin resistance cassette inserted downstream of the *gyrA* protein-coding region	This work
SL1344 *gyrB*::*kan*	Kanamycin resistance cassette inserted downstream of the *gyrB* protein-coding region	This work
SL1344 *gyrBA*	*gyrBA* operon under the control of the *gyrB* promoter, P_{gyrB}	This work
SL1344 *prgH*::*gfp*$^+$	*prgH-gfp*$^+$ *[*LVA]/R::*cat/* fusion of a*gfp*$^+$ gene encoding a destabilized version of GFP to the SPI-1 promoter, P_{prgH}	Ibarra et al. (2010)
SL1344 *gyrBA prgH*::*gfp*$^+$	Fusion of a *gfp*$^+$ derivative encoding a destabilized version of GFP to the SPI-1 promoter, P_{prgH} in the *gyrBA* background	This work
SL1344 *ssaG*::*gfp*$^+$	*prgH-gfp*$^+$ [LVA]/R::*cat/* fusion of a *gfp*$^+$ derivative encoding a destabilized version of GFP to the SPI-2 promoter, P_{ssaG}	Ibarra et al. (2010)
SL1344 *gyrBA ssaG*::*gfp*$^+$	Fusion of a *gfp*$^+$ derivative encoding a destabilized version of GFP to the SPI-2 promoter, P_{ssaG} in the *gyrBA* background	This work
SL1344 *SL1483*::*cat*	Insertion of a chloramphenicol resistance cassette into the pseudogene *SL1483*	This work
SL1344 *gyrBA SL1483*::*cat*	Insertion of a chloramphenicol resistance cassette into the pseudogene *SL1483* in the *gyrBA* background	This work

TABLE 3 Plasmids used in this study

Plasmid name	Description	Reference
pKD3	Amp^R ($Carb^R$), Cm^R	Datsenko and Wanner (2000)
pKD4	Amp^R ($Carb^R$), Kan^R	Datsenko and Wanner (2000)
pKD46	Amp^R ($Carb^R$), λ Red genes *γ*, *β*, *exo* under the control of an arabinose inducible promoter	Datsenko and Wanner (2000)
pCP20	Amp^R ($Carb^R$), Cm^R, FLP recombinase expressing, temperature-sensitive replicon	Cherepanov and Wackernagel (1995)
pUC18	Amp^R ($Carb^R$)	Yanisch-Perron et al. (1985)

Abbreviations: Amp^R ($Carb^R$), ampicillin (carbenicillin) resistance; Cm^R, chloramphenicol resistance; Kan^R, kanamycin resistance.

4.2 | Bacterial motility assays

Assays were carried out precisely as described to achieve agreement between biological replicates. 0.3% LB agar was melted in a 100 ml bottle in a Tyndall steamer for 50 min, allowed to cool in a 55°C water bath for 20 min, six plates were poured and left to dry near a Bunsen flame for 25 min. One microliter of the bacterial overnight culture was pipetted under the agar surface with two inocula per plate. Plates were placed in a 37°C incubator without stacking to ensure equal oxygen access. After 5 hr, the diameters of the resulting swarm zones were measured and expressed as the ratio of the WT zone to that of the mutant.

4.3 | Competitive fitness assays

Flasks of broth were inoculated with a pair of competing bacterial strains in a 1:1 ratio. Derivatives of each competitor were constructed that carried a chloramphenicol acetyltransferase (*cat*) gene cassette within the transcriptionally silent pseudogene *SL1483*. This *cat* insertion is known to be neutral in its effects on bacterial fitness (Lacharme-Lora et al., 2019) and allows the marked strain to be distinguished from its unmarked competitor. Competitions were run in which wild-type SL1344 was the marked strain or in which SL1344 *gyrBA* was the marked strain. Strains to be competed were pre-conditioned in separate 25 ml of cultures for 24 hr without antibiotics. Then 10^5 cells of each strain were mixed in 25 ml of fresh LB broth and grown as a mixed culture for another 24 hr. The number of colony-forming units was determined by plating the mixture on chloramphenicol-containing plates and on plates with no antibiotic at T = 0 hr and T = 24 hr. Taking the wild-type SL1344 versus SL1344 *gyrBA* competition as an example, SL1344 was competed against SL1344 *gyrBA SL1483*::*cat* and, as a control, SL1344_*SL1483*::*cat* was competed against SL1344 *gyrBA*. The competitive fitness index (f.i.) was calculated according to the formula:

$$\text{f.i.} = (\ln(\text{Nc}(24)/\text{Nc}(0))) / (\ln((\text{Nwt}(24)/\text{Nwt}(0)))),$$

where Nc(0) and Nc(24) are the initial and final counts of a competitor and Nwt(0) and Nwt(24) are initial and final counts of the WT. Competitor is a strain other than the WT; f.i. < 1 means that the competitor is less fit than the WT; f.i. > 1 indicates the opposite.

4.4 | *Construction of a* gyrBA *operon strain*

A derivative of *S*. Typhimurium with an artificial *gyrBA* operon was constructed by Lambda-Red homologous recombination (Datsenko & Wanner, 2000). Briefly, a *kan* cassette was amplified from plasmid pKD4 with primers Kan ins gyrA F and Kan ins gyrA R, (Table S1) using Phusion high-fidelity DNA polymerase. The amplicon, with overhangs homologous to a region immediately downstream of *gyrA*, was transformed into the WT strain harboring plasmid pKD46 (Table 3), then grown in the presence of arabinose to activate the Lambda Red system in order to tag *gyrA* with the *kan* cassette. The *gyrA*::*kan* construct, including 20 nucleotides upstream from the *gyrA* translational start codon, was amplified using primers gyrB.int.gyrA::kan_Pf and gyrB.int.gyrA::kan_Prev (Table S1). The amplicon had overhangs that were homologous to sequences immediately downstream of *gyrB*. This allowed the translation of the GyrA protein from the bicistronic *gyrBA* mRNA because several sequences closely matching to a consensus ribosome binding site (5′-AGGAGG-3′) were located in this 20 bp region. The *gyrA*::*kan* amplicon was inserted by Lambda Red-mediated recombination immediately downstream of the *gyrB* protein-coding region to construct the *gyrBA* operon. The original *gyrA* gene was deleted by an in-frame insertion of a *kan* cassette (Baba et al., 2006). The *kan* resistance cassettes were subsequently eliminated via FLP-mediated site-specific recombination (Cherepanov & Wackernagel, 1995). The resulting *gyrBA* strain had the genes that encode both subunits of DNA gyrase arranged as a bicistronic operon under the control of a common promoter, P_{gyrB} (Table 2).

4.5 | DNA isolation for whole-genome sequencing

To obtain high-quality chromosomal DNA for whole-genome sequencing, a basic phenol-chloroform method was used (Sambrook & Russell, 2006). Two milliliters of an overnight culture were centrifuged at 16,000 x g for 1 min to harvest cells and the cell pellet was

resuspended in 400 μl of TE buffer pH 8 (100 mM Tris-HCl pH 8.0, 10 mM EDTA pH 8.0 (BDH, Poole, England)). One percent SDS and 2 mg/ml of proteinase K were added and incubated for 2 hr at 37°C to complete lysis. DNA was isolated by the addition of 1 volume of phenol pH 8.0:chloroform:isoamyl alcohol (25:24:1) (AppliChem, Darmstadt, Germany), thorough mixing and centrifugation at 16,000 ×*g* for 15 min at 4°C in the phase-lock tube. The upper aqueous layer containing DNA was collected and the phenol: chloroform extraction was repeated two more times. To remove contaminants and to precipitate DNA, sodium acetate pH 5.2 at 0.3 M and isopropanol at 60% of the final volume were added and kept for 1 hr at −20°C. DNA was pelleted by centrifugation at 16,000 ×*g* for 15 min at 4°C. The DNA pellet was washed with 70% ethanol, dried at 37°C until translucent, and resuspended in 100 μl of TE pH 8.0. The sample was electrophoresed on the agarose gel to check for degradation and the DNA concentration was determined as follows: to remove RNA contamination from DNA samples, 100 mg/ml of RNase A was added and incubated for 30 min at 37°C. Phenol-chloroform extraction was performed as above. To precipitate DNA, 0.5 M of ammonium acetate (Merck, Darmstadt, Germany) and a half volume of isopropanol were added and incubated for 2 hr at −20°C. DNA was pelleted by centrifugation at 16,000 ×*g* for 15 min at 4°C. The DNA pellet was washed twice with 70% ethanol, dried at 37°C until translucent, and resuspended in 50 μl of water. The sample was run on an agarose gel to check for degradation. The concentration of DNA extracted was determined by measuring absorbance at 260 nm on a DeNovix DS-11 spectrophotometer (Wilmington, Delaware, USA). The shape of the absorbance curve was ensured to have a clear peak at 260 nm. The purity of samples was assessed by the ratio of A_{260}/A_{280} – a measure of protein and phenol contamination and A_{260}/A_{230} – a measure of contaminants such as EDTA, where both should be as close as possible to 2. Only high-quality samples were chosen for further work.

4.6 | Whole-genome sequencing

Whole-genome sequencing was performed on final versions of the constructed strains to ensure that no compensatory mutations were introduced into their genomes. The sequencing was performed by MicrobesNG (Birmingham, UK) using Illumina next-generation sequencing technology. The output reads were assembled using Velvet (Zerbino, 2010) and aligned to the reference SL1344 sequence NC_016810.1 Breseq software (Deatherage & Barrick, 2014). The data are available through the Sequence Read Archive (SRA) with accession number PRJNA682874.

4.7 | *RNA extraction, DNase treatment, and RT-qPCR*

RNA for measuring gene expression by qPCR was isolated using an acidic phenol-chloroform method. An overnight culture was subcultured into 25 ml of fresh LB broth normalizing to an OD600 of 0.003. The bacterial culture was grown to the required timepoint and mixed with 40% volume of 5% acidic phenol (pH 4.3) in ethanol and placed on ice for at least 30 min to stop transcription. The cells were harvested by centrifugation at 3,220 ×*g* for 10 min at 4°C and resuspended in 700 μl of TE buffer pH 8 containing 0.5 mg/ml of lysozyme. One percent SDS and 0.1 mg/ml of proteinase K were added and incubated for 20 min at 40°C to complete lysis. 1/10 volume of 3 M sodium acetate was added to precipitate RNA, 1 volume of 1:1 solution of acidic phenol and chloroform was added, mixed well on a vortex mixer, and centrifuged at 16,000 ×*g* for 15 min at 4°C to extract RNA into the aqueous phase. To precipitate RNA the aqueous layer was harvested, mixed with 1 volume of isopropanol, and incubated at −20°C for 1 hr. RNA was harvested by centrifugation at 16,000 ×*g* for 15 min at 4°C. The RNA pellet was washed with 70% ethanol and dried at 37°C until translucent. The total RNA was dissolved in 50 μl of DEPC-treated water and its concentration was determined using DeNovix DS-11 spectrophotometer.

For DNase-treatment, RNA was diluted to 20 μg in 80 μl, denatured at 65°C for 5 min, and kept on ice. 1x DNase I buffer including MgCl2 and 10 U DNase I (Thermo Fisher Scientific, Waltham, US) were added and incubated for 45 min at 37°C. Hundred microliters of 1:1 acidic phenol : chloroform were added to DNase I digestion samples, mixed and transferred to a phase-lock tube. RNA was extracted by centrifugation at 16,000 ×*g* for 12 min at 15°C. The upper aqueous layer was harvested and RNA was precipitated by adding 2.5 volumes of 30:1 ethanol : 3 M sodium acetate pH 6.5 for 2 hr or overnight at −20°C. RNA was harvested by centrifugation at 16,000 ×*g* for 30 min at 4°C. The RNA pellet was washed with 70% ethanol and dried at 37°C until translucent. The total RNA was dissolved in 30 μl of DEPC-treated water and its concentration was determined as in 2.5.5. RNA was checked for DNA contamination by the end point PCR and for integrity on an HT gel (Mansour & Pestov, 2013).

400 nm of the total extracted and DNase I treated RNA was converted to cDNA using GoScriptTM Reverse Transcription System kit (Promega) according to manufacturer's guidelines. Then, 5.33 ng of cDNA in 20 μl reaction was used as a template for Real-Time quantitative PCR (RT-qPCR) using 1× FastStart Universal SYBR Green Master (ROX) (Roche, Mannheim, Germany) and gene-specific pair of primers (0.3 μM each). For each pair of primers, a standard curve was generated using 10-fold serially diluted gDNA. PCR and fluorescence detection were carried out in StepOne Real-Time PCR system (Applied Biosystems). Analysis was performed in the accompanying software. The cycling conditions were as follows:

10 min at 95°C; 40 cycles of 15 s at 95°C and 1 min at 60°C

4.8 | Minimum inhibitory concentration (MIC) of antibiotics determination

MIC90 of antibiotics (a minimal concentration at which 90% of bacterial growth is inhibited) was found by serially diluting antibiotics and spectrophotometrically testing the ability of different dilutions

to inhibit bacterial growth. On a 96-well plate, all wells (excluding column 12) were filled with 60 μl of sterile LB broth. One milliliter of solutions of antibiotics to be tested was prepared at the highest desired concentration in LB. Three hundred microliters of the prepared antibiotics were added to the wells of column 12 and homogenized by pipetting up and down five times with a multichannel pipette. Two hundred and forty microliters were transferred to the next wells in column 11, homogenization was repeated and serial 1:1.25 dilutions were sequentially continued until column 3. The final 240 μl from column 3 were discarded. All the wells were inoculated with bacterial cultures adjusted to an OD_{600} of 0.003 except column 1. In this way, column 1 contained negative controls (no bacteria and no antibiotic), column 2 contained positive controls (no antibiotics), and columns 3–12 contained serially diluted antibiotics inoculated with the identical number of bacteria. The plate was covered, sealed between plastic sheets, and incubated for 18 hr at the standard growth conditions. The plate was read by measuring OD_{600} values on a plate reader (Multiskan EX, Thermo Electronics).

4.9 | SPI-1 and SPI-2 reporter assays

Salmonella pathogenicity island (SPI) activity was accessed by measuring the expression of gfp^+ reporter gene fusions to promoters of *prgH* and *ssaG* to look at SPI-1 and SPI-2 expression, respectively. The gfp^+ reporter fusions were transduced into each strain by P22 generalized transduction and selected with chloramphenicol. Hundred microliters of the overnight culture of the gfp^+ reporter-carrying strain were diluted 1:100 in LB broth. Black 96 plate with transparent flat bottom was filled with 100 μl of the diluted culture in six technical replicates, negative controls were included. The plate was sealed with parafilm and incubated at 300 rpm, 37°C for 24 hr in the Synergy H1 microplate reader (BioTek, Vermont, USA). Bacterial growth was measured at 600 nm and GFP fluorescence was read using 485.5 nm excitation frequency at 528 nm emission frequency, measurements were taken every 20 min. For measurements in the minimal medium, the culture was adjusted to OD_{600} of 0.03 in the medium of the required $MgCl_2$ concentration, and measurements proceeded as above.

4.10 | Global supercoiling determination

Global DNA supercoiling was assayed in bacterial strains transformed with a reporter plasmid pUC18 (Table 3). An overnight culture of pUC18-containing strain was adjusted to an OD_{600} of 0.003 and grown to the late stationary growth stage (24 hr) in 25 ml of LB broth or in 25 ml of minimal medium N of the required $MgCl_2$ concentration pre-conditioned as above. Fourteen OD_{600} units (6 OD_{600} units for minimal medium) were harvested and pUC18 was isolated with the aid the of QIAprep Spin Miniprep kit (QIAGEN, Hilden, Germany) according to manufacturer's guidelines.

To observe the range of DNA supercoiling states characteristic of a strain at a given growth stage, extracted pUC18 samples were resolved on 0.8% agarose gel supplemented with the DNA intercalating agent chloroquine. Two liters of 1× TBE buffer (89 mM Tris base, 89 mM boric acid, 2 mM EDTA pH 8.0) and 1 ml of 25 mg/ml of chloroquine were made. 0.8% agarose solution was made from 300 μl of TBE and melted in a Tyndall steamer. When the gel cooled down, it was supplemented with 2.5 μg/ml of chloroquine. The 27 cm long gel was poured, left to polymerise for 2 hr, and covered with 1.7 liters of the running buffer containing 1x TBE and chloroquine at 2.5 μg/ml. One microgram or 500 ng of the plasmid samples in 15 μl volumes was mixed with 5x loading dye (80% glycerol, 0.01% bromophenol blue) and loaded on a gel. The gel was electrophoresed for 16 hr at 100 V. The gel was washed in distilled water for 24 hr changing water a few times, stained in 1 μg/ml of ethidium bromide for 1 hr rocking in the dark. The stain was poured off and the gel was washed in distilled water for further 1 hr. The plasmid topoisomers were visualized under UV on the ImageQuant LAS 4,000 imager. ImageJ software was used to outline plasmid topoisomer distribution profiles.

4.11 | Determining the patterns of *gyrA* and *gyrB* locations in bacterial chromosomes

The location of *oriC* in each organism examined was determined using the DoriC 10.0 database (tubic.org/doric) (Luo & Gao, 2019) and the coordinates of their *gyrA* and *gyrB* genes were obtained using the Ensembl bacteria browser (bacteria.ensembl.org). Distance in base pairs between the *oriC* and the gene was calculated and converted into the percentage of the total chromosome size. An attempt was made to cover bacterial taxonomy as broadly as possible, encompassing members of the major bacterial phyla, well studied, and clinically important organisms in the analysis (Table 1). The table is neither complete nor does it claim to include all the existing possibilities of *gyrA* and *gyrB* arrangements in bacterial chromosomes, but instead, exemplifies the arrangement possibilities mentioned in this work. Closely related species and those belonging to the less diverse phyla were found to share the chromosomal positions of *gyrA* and *gyrB* frequently. Thus, one representative of a taxonomic rank was often deemed sufficient for the purpose of inclusion in the table. Lower classification ranks were analyzed within more diverse and studied phyla (Table 1).

4.12 | Mammalian cell culture conditions

RAW264.7 murine macrophages were maintained in Dulbecco's Modified Eagle's Medium (DMEM), (Sigma, catalog number D6429) supplemented with 10% fetal bovine serum (FBS) in a humidified 37°C, 5% CO_2 tissue-culture incubator grown in 75 cm^3 tissue-culture flasks. When approximately 80% confluent growth was achieved, cells were split into a fresh flask. Cells within the 9–16

passage number range were used for infections. All media and PBS used for cell culture were pre-warmed to 37°C. To split cells, old DMEM was removed and the monolayer was rinsed with 10 ml of sterile PBS. Ten milliliters of fresh DMEM were pipetted into the flask and the monolayer was scraped gently with a cell scraper to dislodge the cells. Scraped cells were centrifuged at 450 x g for 5 min in an Eppendorf 5810R centrifuge and the cell pellet was resuspended in 5 ml of DMEM + FBS. One milliliter of the cell suspension was added to 14 ml of fresh DMEM + FBS in a 75 cm^3 flask, gently rocked to mix, and incubated at 37°C, 5% CO_2. To seed cells for infection, cells were treated as for splitting. After resuspension in 5 ml of DMEM + FBS, viable cells were counted on a haemocytometer using trypan blue exclusion dye. A 24-well tissue culture plate was filled with 500 µl of DMEM + FBS. 1.5×10^5 cells were added to each well, gently rocked to mix, and incubated at 37°C, 5% CO_2 for 24 hr.

4.13 | Macrophage viability assay in SPI-1 inducing conditions

Overnight bacterial cultures were subcultured 1:33 in 10 ml of fresh LB broth in 125 ml conical flask and grown for 3.5 hr to maximize SPI-1 expression (Steele-Mortimer et al., 1999). Five hundred microliters of the culture were centrifuged at 16,000 ×*g* for 1 min and resuspended in 500 µl of HBSS−/−. Monolayers were washed twice with 500 µl of HBSS+/+ and infected with bacteria at MOI of five in three technical replicates for each timepoint and strain. The plate was centrifuged at 200 ×*g* for 10 min to synchronize infections and incubated for 30 min at 37°C, 5% CO_2. In the meantime, the infection medium was plated for enumeration on LB agar plates—T = 0 hr. Gentamicin protection assay was used to determine bacterial counts inside macrophages. To kill all extracellular bacteria, the monolayers were washed once with HBSS+/+ and high gentamicin (100 µg/ml) treatment diluted in DMEM + FBS was added to the wells. The plate was incubated at 37°C, 5% CO_2 for 1 hr. At 1 hr post-infection, the monolayers were washed three times with HBSS+/+, macrophages were lysed by adding 1 ml of ice-cold water, pipetting up and down ten times with scraping and intracellular bacteria were plated for enumeration. The monolayers which were intended for other timepoints were washed once with HBSS+/+, low gentamicin (10 µg/ml) treatment in DMEM + FBS was added and the plate was incubated at 37°C, 5% CO_2. The low gentamicin concentration is to ensure that any extracellular bacteria are killed, but at the same time to avoid gentamicin permeabilizing the plasma membrane of a macrophage (Kaneko et al., 2016). At later timepoints monolayers were washed three times with HBSS+/+, macrophages were lysed by adding 1 ml of ice-cold water, pipetting up and down ten times with scraping and intracellular bacteria were plated for enumeration.

ACKNOWLEDGMENTS

Research in the CJD laboratory is supported by Science Foundation Ireland Investigator Award 13/IA/1875.

CONFLICTS OF INTEREST

The authors declare that they have no conflicts of interest.

ORCID

Charles J. Dorman https://orcid.org/0000-0002-6018-9170

REFERENCES

Ahmed, W., Menon, S., Karthik, P.V. and Nagaraja, V. (2016) Autoregulation of topoisomerase I expression by supercoiling sensitive transcription. *Nucleic Acids Research*, *44*, 1541–1552.

Ahmed, W., Sala, C., Hegde, S.R., Jha, R.K., Cole, S.T. and Nagaraja, V. (2017) Transcription facilitated genome-wide recruitment of topoisomerase I and DNA gyrase. *PLoS Genetics*, *13*, 1–20. https://doi.org/10.1371/journal.pgen.1006754.

Alokam, S., Liu, S.L., Said, K. and Sanderson, K.E. (2002) Inversions over the terminus region in *Salmonella* and *Escherichia coli*: IS*200*s as the sites of homologous recombination inverting the chromosome of *Salmonella enterica* serovar Typhi. *Journal of Bacteriology*, *184*, 6190–6197. https://doi.org/10.1128/JB.184.22.6190-6197.2002.

Ashley, R.E., Dittmore, A., McPherson, S.A., Turnbough, C.L. Jr, Neuman, K.C. and Osheroff, N. (2017) Activities of gyrase and topoisomerase IV on positively supercoiled DNA. *Nucleic Acids Research*, *45*, 9611–9624.

Baba, T., Ara, T., Hasegawa, M., Takai, Y., Okumura, Y., Baba, M. et al (2006) Construction of *Escherichia coli* K-12 in-frame, single-gene knockout mutants: the Keio collection. *Molecular Systems Biology*, *2*(2006), 8.

Baba, T., Bae, T., Schneewind, O., Takeuchi, F. and Hiramatsu, K. (2008) Genome sequence of *Staphylococcus aureus* strain Newman and comparative analysis of Staphylococcal genomes; polymorphism and evolution of two major pathogenicity Islands. *Journal of Bacteriology*, *190*, 300–310. https://doi.org/10.1128/JB.01000-07.

Banda, M.M., Zavala-Alvarado, C., Perez-Morales, D. and Bustamante, V.H. (2019) SlyA and HilD counteract H-NS-mediated repression on the *ssrAB* virulence operon of *Salmonella enterica* serovar Typhimurium and thus promote its activation by OmpR. *Journal of Bacteriology*, *201*, e00530–e618.

Bates, A.D. and Maxwell, A. (2005) *DNA Topology*. Oxford University Press.

Berger, J.M. (1998) Type II DNA topoisomerases. *Current Opinion in Structural Biology*, *8*, 26–32. https://doi.org/10.1016/S0959-440X(98)80006-7.

Berlyn, M.K. (1998) Linkage map of *Escherichia coli* K-12, edition 10: the traditional map. *Microbiology and Molecular Biology Reviews*, *62*, 814–984. https://doi.org/10.1128/MMBR.62.3.814-984.1998.

Blattner, F.R., Plunkett, G. III, Bloch, C.A., Perna, N.T., Burland, V., Riley, M. et al (1997) The complete genome sequence of *Escherichia coli* K-12. *Science*, *277*, 1453–1474. https://doi.org/10.1126/science.277.5331.1453.

Bliska, J.B. and Cozzarelli, N.R. (1987) Use of site-specific recombination as a probe of DNA structure and metabolism *in vivo*. *Journal of Molecular Biology*, *194*, 205–218. https://doi.org/10.1016/0022-2836(87)90369-X.

Bogue, M.M., Mogre, A., Beckett, M.C., Thomson, N.R. and Dorman, C.J. (2020) Network rewiring: physiological consequences of reciprocally exchanging the physical locations and growth-phase-dependent expression patterns of the *Salmonella* Fis and Dps Genes. *mBio*, *11*, e0218–e220.

Bryant, J.A., Sellars, L.E., Busby, S.J. and Lee, D.J. (2014) Chromosome position effects on gene expression in *Escherichia coli* K-12. *Nucleic Acids Research*, *42*, 11383–11392. https://doi.org/10.1093/nar/gku828.

Bush, N.G., Diez-Santos, I., Abbott, L.R. and Maxwell, A. (2020) Quinolones: mechanism, lethality and their contributions to antibiotic resistance. *Molecules*, *25*, 5662. https://doi.org/10.3390/molecules25235662.

Cameron, A.D. and Dorman, C.J. (2012) A fundamental regulatory mechanism operating through OmpR and DNA topology controls expression of *Salmonella* pathogenicity islands SPI-1 and SPI-2. *PLoS Genetics*, *8*, e1002615. https://doi.org/10.1371/journal.pgen.1002615.

Cameron, A.D., Stoebel, D.M. and Dorman, C.J. (2011) DNA supercoiling is differentially regulated by environmental factors and FIS in *Escherichia coli* and *Salmonella enterica*. *Molecular Microbiology*, *80*, 85–101. https://doi.org/10.1111/j.1365-2958.2011.07560.x.

Champion, K. and Higgins, N.P. (2007) Growth rate toxicity phenotypes and momeostatic supercoil control differentiate *Escherichia coli* from *Salmonella enterica* serovar Typhimurium. *Journal of Bacteriology*, *189*, 5839–5849.

Cherepanov, P.P. and Wackernagel, W. (1995) Gene disruption in *Escherichia coli*: TcR and KmR cassettes with the option of Flp-catalyzed excision of the antibiotic-resistance determinant. *Gene*, *158*, 9–14. https://doi.org/10.1016/0378-1119(95)00193-A.

Cheung, K.J., Badarinarayana, V., Selinger, D.W., Janse, D. and Church, G.M. (2003) A microarray-based antibiotic screen identifies a regulatory role for supercoiling in the osmotic stress response of *Escherichia coli*. *Genome Research*, *13*, 206–215. https://doi.org/10.1101/gr.401003.

Chong, S., Chen, C., Ge, H. and Xie, X.S. (2014) Mechanism of transcriptional bursting in bacteria. *Cell*, *158*, 314–326. https://doi.org/10.1016/j.cell.2014.05.038.

Colgan, A.M., Quinn, H.J., Kary, S.C., Mitchenall, L.A., Maxwell, A., Cameron, A.D.S. et al (2018) Negative supercoiling of DNA by gyrase is inhibited in *Salmonella enterica* serovar typhimurium during adaptation to acid stress. *Molecular Microbiology*, *107*, 734–746. https://doi.org/10.1111/mmi.13911.

Conter, A., Menchon, C. and Gutierrez, C. (1997) Role of DNA supercoiling and *rpoS* sigma factor in the osmotic and growth phase-dependent induction of the gene *osmE* of *Escherichia coli* K12. *Journal of Molecular Biology*, *273*, 75–83. https://doi.org/10.1006/jmbi.1997.1308.

Cooper, S. and Helmstetter, C.E. (1968) Chromosome replication and the division cycle of *Escherichia coli* B/r. *Journal of Molecular Biology*, *31*, 519–540. https://doi.org/10.1016/0022-2836(68)90425-7.

Corbett, K.D. and Berger, J.M. (2004) Structure, molecular mechanisms, and evolutionary relationships in DNA topoisomerases. *Annual Review of Biophysics and Biomolecular Structure*, *33*, 95–118. https://doi.org/10.1146/annurev.biophys.33.110502.140357.

O Cróinín, T., Carroll, R.K., Kelly, A. and Dorman, C.J. (2006) Roles for DNA supercoiling and the Fis protein in modulating expression of virulence genes during intracellular growth of *Salmonella enterica* serovar Typhimurium. *Molecular Microbiology*, *62*, 869–882. https://doi.org/10.1111/j.1365-2958.2006.05416.x.

Dandekar, T., Snel, B., Huynen, M. and Bork, P. (1998) Conservation of gene order: a fingerprint of proteins that physically interact. *Trends in Biochemical Sciences*, *23*, 324–328. https://doi.org/10.1016/S0968-0004(98)01274-2.

Datsenko, K.A. and Wanner, B.L. (2000) One-step inactivation of chromosomal genes in Escherichia coli K-12 using PCR products. *Proceedings of the National Academy of Sciences of the United States of America.*, *97*, 6640–6645. https://doi.org/10.1073/pnas.120163297.

de Daruvar, A., Collado-Vides, J. and Valencia, A. (2002) Analysis of the cellular functions of *Escherichia coli* operons and their conservation in *Bacillus subtilis*. *Journal of Molecular Evolution*, *55*, 211–221. https://doi.org/10.1007/s00239-002-2317-1.

Deatherage, D.E. and Barrick, J.E. (2014) Identification of mutations in laboratory-evolved microbes from next-generation sequencing data using breseq. *Methods in Molecular Biology*, *1151*, 165–188.

Dekker, N.H., Rybenkov, V.V., Duguet, M., Crisona, N.J., Cozzarelli, N.R., Bensimon, D., et al (2002) The mechanism of type IA topoisomerases. *Proceedings of the National Academy of Sciences of the United States of America*, *99*, 12126–12131. https://doi.org/10.1073/pnas.132378799.

Dillon, S.C. and Dorman, C.J. (2010) Bacterial nucleoid-associated proteins, nucleoid structure and gene expression. *Nature Reviews Microbiology*, *8*, 185–195. https://doi.org/10.1038/nrmicro2261.

DiNardo, S., Voelkel, K.A., Sternglanz, R., Reynolds, A.E. and Wright, A. (1982) *Escherichia coli* DNA topoisomerase I mutants have compensatory mutations in DNA gyrase genes. *Cell*, *31*, 43–51. https://doi.org/10.1016/0092-8674(82)90403-2.

Dorman, C.J. (2019) DNA supercoiling and transcription: a two-way street. *BMC Molecular and Cell Biology*, *20*, 26–39. https://doi.org/10.1186/s12860-019-0211-6.

Dorman, C.J. and Dorman, M.J. (2016) DNA supercoiling is a fundamental regulatory principle in the control of bacterial gene expression. *Biophysical Reviews*, *8*, 209–220. https://doi.org/10.1007/s12551-016-0205-y.

Dorman, C.J., Lynch, A.S., Ní Bhriain, N. and Higgins, C.F. (1989) DNA supercoiling in *Escherichia coli*: *topA* mutations can be suppressed by DNA amplifications involving the *tolC* locus. *Molecular Microbiology*, *3*, 531–540. https://doi.org/10.1111/j.1365-2958.1989.tb00199.x.

Drlica, K. & Zhao, X. (1997) DNA gyrase, topoisomerase IV, and the 4-quinolones. *Microbiology and Molecular Biology Reviews*, *61*, 377–392. https://doi.org/10.1128/.61.3.377-392.1997.

Fass, E. and Groisman, E.A. (2009) Control of *Salmonella* pathogenicity island-2 gene expression. *Current Opinion in Microbiology*, *12*, 199–204. https://doi.org/10.1016/j.mib.2009.01.004.

Figueira, R. and Holden, D.W. (2012) Functions of the *Salmonella* pathogenicity island 2 (SPI-2) type III secretion system effectors. *Microbiology*, *158*, 1147–1161. https://doi.org/10.1099/mic.0.058115-0.

Forterre, P., Gribaldo, S., Gadelle, D. and Serre, M.C. (2007) Origin and evolution of DNA topoisomerases. *Biochimie*, *89*, 427–446. https://doi.org/10.1016/j.biochi.2006.12.009.

Garvis, S.G., Beuzón, C.R. and Holden, D.W. (2001) A role for the PhoP/Q regulon in inhibition of fusion between lysosomes and *Salmonella*-containing vacuoles in macrophages. *Cellular Microbiology*, *3*, 731–744.

Gellert, M., Mizuuchi, K., O'Dea, M.H., Itoh, T. and Tomizawa, J.I. (1977) Nalidixic acid resistance: A second genetic character involved in DNA gyrase activity. *Proceedings of the National Academy of Sciences of the United States of America*, *74*, 4772–4776. https://doi.org/10.1073/pnas.74.11.4772.

Gellert, M., Mizuuchi, K., O'Dea, M.H. and Nash, H.A. (1976) DNA gyrase: enzyme that introduces superhelical turns into DNA. *Proceedings of the National Academy of Sciences of the United States of America*, *73*, 3872–3876.

Gerganova, V., Berger, M., Zaldastanishvili, E., Sobetzko, P., Lafon, C., Mourez, M. et al (2015) Chromosomal position shift of a regulatory gene alters the bacterial phenotype. *Nucleic Acids Research*, *43*, 8215–8226. https://doi.org/10.1093/nar/gkv709.

Glaser, P., Frangeul, L., Buchrieser, C., Rusniok, C., Amend, A., Baquero, F. et al (2001) Comparative genomics of *Listeria* species. *Science*, *294*, 849–852.

Hensel, M. (2000) *Salmonella* pathogenicity island 2. *Molecular Microbiology*, *36*, 1015–1023. https://doi.org/10.1046/j.1365-2958.2000.01935.x.

Higgins, N.P. (2014) RNA polymerase: chromosome domain boundary maker and regulator of supercoil density. *Current Opinion in Microbiology*, *22*, 138–143. https://doi.org/10.1016/j.mib.2014.10.002.

Higgins, N.P. (2016) Species-specific supercoil dynamics of the bacterial nucleoid. *Biophysical Reviews*, *8*, 113–121. https://doi.org/10.1007/s12551-016-0207-9.

Higgins, N.P., Peebles, C.L., Sugino, A. and Cozzarelli, N.R. (1978) Purification of subunits of *Escherichia coli* DNA gyrase and reconstitution of enzymatic activity. *Proceedings of the National Academy of Sciences of the United States of America*, *75*, 1773–1777. https://doi.org/10.1073/pnas.75.4.1773.

Hoiseth, S.K. and Stocker, B.A. (1981) Aromatic-dependent *Salmonella* Typhimurium are non-virulent and effective as live vaccines. *Nature*, *291*, 238–239. https://doi.org/10.1038/291238a0.

Ibarra, J.A., Knodler, L.A., Sturdevant, D.E., Virtaneva, K., Carmody, A.B., Fischer, E.R. et al (2010) Induction of *Salmonella* pathogenicity island 1 under different growth conditions can affect *Salmonella*-host cell interactions *in vitro*. *Microbiology*, *156*, 1120–1133. https://doi.org/10.1099/mic.0.032896-0.

Kaneko, M., Emoto, Y. and Emoto, M. (2016) A simple, reproducible, inexpensive, yet old-fashioned method for determining phagocytic and bactericidal activities of macrophages. *Yonsei Medical Journal*, *57*, 283–290. https://doi.org/10.3349/ymj.2016.57.2.283.

Keane, O.M. and Dorman, C.J. (2003) The *gyr* genes of *Salmonella enterica* serovar Typhimurium are repressed by the factor for inversion stimulation, Fis. *Molecular Genetics and Genomics*, *270*, 56–65. https://doi.org/10.1007/s00438-003-0896-1.

Klostermeier, D. (2018) Why two? On the role of (A-)symmetry in negative supercoiling of DNA by gyrase. *International Journal of Molecular Sciences*, *19*, 1489.–https://doi.org/10.3390/ijms19051489.

Kröger, C., Colgan, A., Srikumar, S., Händler, K., Sivasankaran, S.K., Hammarlöf, D.L., et al. (2013) An infection-relevant transcriptomic compendium for Salmonella enterica serovar Typhimurium. *Cell Host Microbe*, *14*, 683–695. https://doi.org/10.1016/j.chom.2013.11.010.

Lacharme-Lora, L., Owen, S.V., Blundell, R., Canals, R., Wenner, N., Perez-Sepulveda, B. et al (2019) The use of chicken and insect infection models to assess the virulence of African *Salmonella* Typhimurium ST313. *PLoS Neglected Tropical Diseases*, *13*, e0007540.

Lawrence, J.G. and Roth, J.R. (1996) Selfish operons: horizontal transfer may drive the evolution of gene clusters. *Genetics*, *143*, 1843–1860. https://doi.org/10.1093/genetics/143.4.1843.

Le, T.B. and Laub, M.T. (2016) Transcription rate and transcript length drive formation of chromosomal interaction domain boundaries. *EMBO Journal*, *35*, 1582–1595. https://doi.org/10.15252/embj.201593561.

Letunic, I. & Bork, P. (2019) Interactive tree of life (iTOL) v4: recent updates and new developments. *Nucleic Acids Research*, *47*, W256–W259. https://doi.org/10.1093/nar/gkz239.

Lewis, R.J., Singh, O.M., Smith, C.V., Skarzynski, T., Maxwell, A., Wonacott, A.J. et al (1996) The nature of inhibition of DNA gyrase by the coumarins and the cyclothialidines revealed by X-ray crystallography. *EMBO Journal*, *15*, 1412–1420. https://doi.org/10.1002/j.1460-2075.1996.tb00483.x.

Li, G.W., Burkhardt, D., Gross, C. and Weissman, J.S. (2014) Quantifying absolute protein synthesis rates reveals principles underlying allocation of cellular resources. *Cell*, *157*, 624–635. https://doi.org/10.1016/j.cell.2014.02.033.

Liu, L.F. and Wang, J.C. (1987) Supercoiling of the DNA template during transcription. *Proceedings of the National Academy of Sciences of the United States of America*, *84*, 7024–7027. https://doi.org/10.1073/pnas.84.20.7024.

Luo, H. and Gao, F. (2019) DoriC 10.0: an updated database of replication origins in prokaryotic genomes including chromosomes and plasmids. *Nucleic Acids Research*, *47*, D74–D77.

Mangan, M.W., Lucchini, S., Danino, V., Croinin, T.O., Hinton, J.C.D. & Dorman, C.J. (2006) The integration host factor (IHF) integrates stationary-phase and virulence gene expression in *Salmonella enterica* serovar Typhimurium. *Molecular Microbiology*, *59*, 1831–1847. https://doi.org/10.1111/j.1365-2958.2006.05062.x.

Mangan, M.W., Lucchini, S., Ó Cróinín, T., Fitzgerald, S., Hinton, J.C.D. and Dorman, C.J. (2011) Nucleoid-associated protein HU controls three regulons that coordinate virulence, response to stress and general physiology in *Salmonella enterica* serovar Typhimurium. *Microbiology*, *157*, 1075–1087. https://doi.org/10.1099/mic.0.046359-0.

Mansour, F.H. and Pestov, D.G. (2013) Separation of long RNA by agarose-formaldehyde gel electrophoresis. *Analytical Biochemistry*, *441*, 18–20. https://doi.org/10.1016/j.ab.2013.06.008.

Martín, C.M., Zaritsky, A., Fishov, I. & Guzmán, E.C. (2020) Transient enhanced cell division by blocking DNA synthesis in *Escherichia coli*. *Microbiology*, *166*, 516–521.

McClelland, M., Sanderson, K.E., Spieth, J., Clifton, S.W., Latreille, P., Courtney, L. et al (2001) Complete genome sequence of *Salmonella enterica* serovar Typhimurium LT2. *Nature*, *413*, 852–856.

Menzel, R. and Gellert, M. (1983) Regulation of the genes for *E. coli* DNA gyrase: homeostatic control of DNA supercoiling. *Cell*, *34*, 105–113. https://doi.org/10.1016/0092-8674(83)90140-X.

Menzel, R. and Gellert, M. (1987) Modulation of transcription by DNA supercoiling: a deletion analysis of the *Escherichia coli gyrA* and *gyrB* promoters. *Proceedings of the National Academy of Sciences of the United States of America*, *84*, 4185–4189. https://doi.org/10.1073/pnas.84.12.4185.

Miller, J.F. (1972) *Experiments in molecular genetics*. Cold Spring Harbor Laboratory Press.

Moffitt, J.R., Pandey, S., Boettiger, A.N., Wang, S. and Zhuang, X. (2016) Spatial organization shapes the turnover of a bacterial transcriptome. *eLife*, *5*, e13065. https://doi.org/10.7554/eLife.13065.

Nelson, D.L. and Kennedy, E.P. (1971) Magnesium transport in *Escherichia coli*. inhibition by cobaltous ion. *Journal of Biological Chemistry*, *246*, 3042–3304. https://doi.org/10.1016/S0021-9258(18)62288-4.

Neumann, S. and Quiñones, A. (1997) Discoordinate gene expression of *gyrA* and *gyrB* in response to DNA gyrase inhibition in *Escherichia coli*. *Journal of Basic Microbiology*, *37*, 53–69. https://doi.org/10.1002/jobm.3620370109.

Nöllmann, M., Stone, M.D., Bryant, Z., Gore, J., Crisona, N.J., Hong, S.-C. et al (2007) Multiple modes of *Escherichia coli* DNA gyrase activity revealed by force and torque. *Nature Structural & Molecular Biology*, *14*, 264–271. https://doi.org/10.1038/nsmb1213.

Pal, C. and Hurst, L.D. (2004) Evidence against the selfish operon theory. *Trends in Genetics*, *20*, 232–234. https://doi.org/10.1016/j.tig.2004.04.001.

Peter, B.J., Arsuaga, J., Breier, A.M., Khodursky, A.B., Brown, P.O. and Cozzarelli, N.R. (2004) Genomic transcriptional response to loss of chromosomal supercoiling in *Escherichia coli*. *Genome Biology*, *5*, R87.

Price, M.N., Arkin, A.P. and Alm, E.J. (2006) The life-cycle of operons. *PLoS Genetics*, *2*, e96.–https://doi.org/10.1371/journal.pgen.0020096.

Price, M.N., Huang, K.H., Alm, E.J. & Arkin, A.P. (2005) Operon formation is driven by co-regulation and not by horizontal gene transfer. *Genome Research*, *15*, 809–819. https://doi.org/10.1101/gr.3368805.

Pruss, G.J., Manes, S.H. and Drlica, K. (1982) *Escherichia coli* DNA topoisomerase I mutants: increased supercoiling is corrected by mutations near gyrase genes. *Cell*, *31*, 35–42. https://doi.org/10.1016/0092-8674(82)90402-0.

Quinn, H.J., Cameron, A.D. and Dorman, C.J. (2014) Bacterial regulon evolution: distinct responses and roles for the identical OmpR proteins of *Salmonella* Typhimurium and *Escherichia coli* in the acid stress response. *PLoS Genetics*, *10*, e1004215. https://doi.org/10.1371/journal.pgen.1004215.

Rahmouni, A.R. and Wells, R.D. (1992) Direct evidence for the effect of transcription on local DNA supercoiling *in vivo*. *Journal of Molecular Biology*, *223*, 131–144. https://doi.org/10.1016/0022-2836(92)90721-U.

Raji, A., Zabel, D.J., Laufer, C.S. and Depew, R.E. (1985) Genetic analysis of mutations that compensate for loss of *Escherichia coli* DNA topoisomerase I. *Journal of Bacteriology*, *162*, 1173–1179. https://doi.org/10.1128/JB.162.3.1173-1179.1985.

Rani, P. and Nagaraja, V. (2019) Genome-wide mapping of Topoisomerase I activity sites reveal its role in chromosome segregation. *Nucleic Acids Research*, *47*, 1416–1427. https://doi.org/10.1093/nar/gky1271.

Richardson, S.M., Higgins, C.F. and Lilley, D.M. (1988) DNA supercoiling and the *leu-500* promoter mutation of *Salmonella typhimurium*. *EMBO Journal*, *7*, 1863–1869. https://doi.org/10.1002/j.1460-2075.1988.tb03019.x.

Rocha, E.P. (2008) The organization of the bacterial genome. *Annual Review of Genetics*, *42*, 211–233. https://doi.org/10.1146/annurev.genet.42.110807.091653.

Rogozin, I.B., Makarova, K.S., Murvai, J., Czabarka, E., Wolf, Y.I., Tatusov, R.L. et al (2002) Connected gene neighborhoods in prokaryotic genomes. *Nucleic Acids Research*, *30*, 2212–2223. https://doi.org/10.1093/nar/30.10.2212.

Sambrook, J. and Russell, D.W. (2006) Purification of nucleic acids by extraction with phenol:chloroform. *Cold Spring Harbor Protocols 2006*. https://doi.org/10.1101/pdb.prot4455.

Schmieger, H. (1972) Phage P22-mutants with increased or decreased transduction abilities. *Molecular and General Genetics*, *119*, 75–88. https://doi.org/10.1007/BF00270447.

Schneider, R., Travers, A., Kutateladze, T. and Muskhelishvili, G. (1999) A DNA architectural protein couples cellular physiology and DNA topology in *Escherichia coli*. *Molecular Microbiology*, *34*, 953–964. https://doi.org/10.1046/j.1365-2958.1999.01656.x.

Scholz, S.A., Diao, R., Wolfe, M.B., Fivenson, E.M., Lin, X.N. and Freddolino, P.L. (2019) High-resolution mapping of the *Escherichia coli* chromosome reveals positions of high and low transcription. *Cell Syst*, *8*, 212–225. https://doi.org/10.1016/j.cels.2019.02.004.

Sharma, B. and Hill, T.M. (1995) Insertion of inverted Ter sites into the terminus region of the *Escherichia coli* chromosome delays completion of DNA replication and disrupts the cell cycle. *Molecular Microbiology*, *18*, 45–61.

Sobetzko, P. (2016) Transcription-coupled DNA supercoiling dictates the chromosomal arrangement of bacterial genes. *Nucleic Acids Research*, *44*, 1514–1524. https://doi.org/10.1093/nar/gkw007.

Sobetzko, P., Travers, A. and and Muskhelishvili, G. (2012) Gene order and chromosome dynamics coordinate spatiotemporal gene expression during the bacterial growth cycle. *Proceedings of the National Academy of Sciences of the United States of America*, *109*, E42–E50. https://doi.org/10.1073/pnas.1108229109.

Steck, T.R., Pruss, G.J., Manes, S.H., Burg, L. and Drlica, K. (1984) DNA supercoiling in gyrase mutants. *Journal of Bacteriology*, *158*, 397–403. https://doi.org/10.1128/JB.158.2.397-403.1984.

Steele-Mortimer, O., Méresse, S., Gorvel, J.P., Toh, B.H. and Finlay, B.B. (1999) Biogenesis of *Salmonella* Typhimurium-containing vacuoles in epithelial cells involves interactions with the early endocytic pathway. *Cellular Microbiology*, *1*, 33–49. https://doi.org/10.1046/j.1462-5822.1999.00003.x.

Stracy, M., Wollman, A.J.M., Kaja, E., Gapinski, J., Lee, J.E., Leek, V.A. et al (2019) Single-molecule imaging of DNA gyrase activity in living *Escherichia coli*. *Nucleic Acids Research*, *47*, 210–220.

Straney, R., Krah, R. and Menzel, R. (1994) Mutations in the -10 TATAAT sequence of the *gyrA* promoter affect both promoter strength and sensitivity to DNA supercoiling. *Journal of Bacteriology*, *176*, 5999–6006. https://doi.org/10.1128/JB.176.19.5999-6006.1994.

Sutormin, D., Rubanova, N., Logacheva, M., Ghilarov, D. and Severinov, K. (2019) Single-nucleotide-resolution mapping of DNA gyrase cleavage sites across the *Escherichia coli* genome. *Nucleic Acids Research*, *47*, 1373–1388.

Swain, P.S. (2004) Efficient attenuation of stochasticity in gene expression through post-transcriptional control. *Journal of Molecular Biology*, *344*, 965–976. https://doi.org/10.1016/j.jmb.2004.09.073.

Tobe, T., Yoshikawa, M. and Sasakawa, C. (1995) Thermoregulation of *virB* transcription in *Shigella flexneri* by sensing of changes in local DNA superhelicity. *Journal of Bacteriology*, *177*, 1094–1097.

Tse-Dinh, Y. and Beran, R. (1988) Multiple promoters for transcription of the *E. coli* DNA topoisomerase I gene and their regulation by DNA supercoiling. *Journal of Molecular Biology*, *202*, 735–742.

Unniraman, S., Chatterji, M. and Nagaraja, V. (2002) DNA gyrase in *Mycobacterium tuberculosis*: A single operon driven by multiple promoters. *Journal of Bacteriology*, *184*, 5449–5456.

Unniraman, S. and Nagaraja, V. (1999) Regulation of DNA gyrase operon in *Mycobacterium smegmatis*: a distinct mechanism of relaxation stimulated transcription. *Genes to Cells*, *4*, 697–706.

van der Heijden, J. & Finlay, B.B. (2012) Type III effector-mediated processes in *Salmonella* infection. *Future Microbiology*, *7*, 685–703.

Weidlich, D. and Klostermeier, D. (2020) Functonal interactions between gyrase subunits are optimized in a species-specific manner. *Journal of Biological Chemistry*, *295*, 22299–22312.

Williams, N.L. and Maxwell, A. (1999) Probing the two-gate mechanism of DNA gyrase using cysteine cross-linking. *Biochemistry*, *38*, 13502–13511.

Wu, H.Y., Shyy, S.H., Wang, J.C. and Liu, L.F. (1988) Transcription generates positively and negatively supercoiled domains in the template. *Cell*, *53*, 433–440. https://doi.org/10.1016/0092-8674(88)90163-8.

Yanisch-Perron, C., Vieira, J. and Messing, J. (1985) Improved M13 phage cloning vectors and host strains: nucleotide sequences of the M13mp18 and pUC19 vectors. *Gene*, *33*, 103–119.

Zerbino, D.R. (2010) Using the Velvet de novo assembler for short-read sequencing technologies. In *Current Protocols in Bioinformatics*. Vol *31*, Chapter, 11, Unit 11.15.https://doi.org/10.1002/0471250953.bi1105s31.

SUPPORTING INFORMATION

Additional Supporting Information may be found online in the Supporting Information section.

How to cite this article: Pozdeev G, Mogre A, Dorman CJ. Consequences of producing DNA gyrase from a synthetic *gyrBA* operon in *Salmonella enterica* serovar Typhimurium. *Mol Microbiol*. 2021;115:1410–1429. https://doi.org/10.1111/mmi.14689